8-2016

Clinical Significance of Homologous Recombination Deficiency Score Testing in Endometrial Cancer

Jean M. Hansen

CLINICAL SIGNIFICANCE OF HOMOLOGOUS RECOMBINATION DEFICIENCY SCORE TESTING IN ENDOMETRIAL CANCER

by

Jean Marie Hansen, DO

APPROVED:

_____
Anil K. Sood, MD
Advisory Professor

_____
Keith Baggerly, PhD

_____
Menashe Bar-Eli, PhD

_____
Junjie Chen, PhD

_____
Xiongbin Lu, PhD

APPROVED:

_____
Dean, The University of Texas
Graduate School of Biomedical Sciences at Houston

CLINICAL SIGNIFICANCE OF HOMOLOGOUS RECOMBINATION DEFICIENCY SCORE TESTING IN ENDOMETRIAL CANCER

A

THESIS

Presented to the Faculty of

The University of Texas

Health Science Center at Houston

Graduate School of Biomedical Sciences

and

The University of Texas MD Anderson Cancer Center

in Partial Fulfillment

of the Requirements

for the Degree of

MASTER OF SCIENCE

by

Jean Marie Hansen, DO

Houston, Texas

August 2016

CLINICAL SIGNIFICANCE OF HOMOLOGOUS RECOMBINATION DEFICIENCY SCORE TESTING IN ENDOMETRIAL CANCER

Jean Marie Hansen, DO

Advisor: Anil K. Sood, MD

Abstract

Objectives: Homologous recombination deficiency (HRD) score is related to chemotherapy response in breast and ovarian cancers. The role of HRD is unknown in endometrial cancer. We examined the relationship between HRD score and survival in a cohort of endometrial cancer patients and with tumor growth using murine orthotopic models.

Methods: TCGA was queried to determine frequency and clinical significance of alterations in the HR pathway in endometrial cancer. 137 formalin-fixed paraffin-embedded endometrioid adenocarcinoma patient samples were tested for HRD score, microsatellite instability (MSI) and high mutation load (HML) using a next generation sequencing assay targeting the coding regions of 43 genes and 54,091 genome wide single nucleotide polymorphisms (SNPs) developed by Myriad Genetics. The HRD score is the sum of three previously described scores (loss of heterozygosity, telomeric allelic imbalance, and large-scale state transition) that quantitate genome rearrangement. Clinical records were obtained. HRD scores were also generated on a panel of established endometrial cancer cell lines and their in vivo growth and

response to olaparib and chemotherapy were assessed. Tumor growth and patterns of metastatic spread were assessed in orthotopic mouse models of endometrial cancer.

Results: Median age at diagnosis was 62 years. The majority of patients presented with early stage disease (54%, 11%, 27%, 8% stage I, II, III, IV respectively), and FIGO grade 2 histology (1%, 73%, 26% grade 1, 2, 3). HRD scores were generated for 112 patient samples, MSI status was determined for 126 samples, and HML status determined for 137 samples. The median HRD score was 3. Patients with HRD score ≥ 10 trended toward worse survival as compared to patients with HRD score <10 (P=0.17). Hec1a cell line (HRD score = 19) was highly sensitive to olaparib and was selected for *in vivo* use. At the time of necropsy, mice injected with Hec1a and treated with PARP inhibitor had significantly decreased tumor growth and HR function as compared with untreated controls, regardless of BRCA1 function.

Conclusions: High HRD score was associated with worse survival in our patient cohort. Our findings support the use of HRD score in guiding the choice of adjuvant therapy for patients with advanced endometrial cancer.

Table of Contents

List of Figures

List of Tables

Introduction

Epidemiology and treatment of endometrial cancer

Endometrial cancer is the most common gynecologic malignancy in the United States and other developed countries, and second most common worldwide [1]. In 2015, an estimated 54,870 women were diagnosed with uterine cancer, and there were an estimated 10,170 deaths from the disease [1]. The most common site of disease in the uterus is the endometrium, and the most common histology is adenocarcinoma. Approximately 80% of endometrial adenocarcinoma cases have endometrioid histology [2], which is the primary focus of the work discussed here. Endometrioid endometrial cancer is graded according to the percentage of solid tumor growth present, with grade 3 histology corresponding with greater than 50% solid tumor growth [3]. The remaining 20% of cases are comprised of non-endometrioid histologies, including serous and clear cell [4,5]. The median age of diagnosis of endometrial cancer is 62 [6], and risk factors for endometrioid endometrial cancer include exposure to unopposed estrogen due to obesity, exogenous estrogen ad ministration, chronic anovulation, and estrogen-secreting tumors [7,8,9,10,11]. Additional risk factors include tamoxifen use [12], early menarche, late menopause [13], and familial cancer syndromes including Cowden and Lynch syndrome [14,15,16].

Patients with endometrial cancer most commonly present with pre-menopausal abnormal uterine bleeding, or post-menopausal bleeding, prompting endometrial sampling via office endometrial biopsy or endometrial curetting [17]. Endometrial cancer is staged surgically via hysterectomy, bilateral salpingo-oophorectomy [18], with the addition of pelvic and para-aortic lymphadenectomy in cases of serous, clear cell or high grade endometrioid histology, tumor size greater than 2 cm, or greater than 50% myometrial invasion on frozen pathology [19,20,21]. Approximately two-thirds of endometrial cancer cases are diagnosed when the disease is confined to the uterus, and five-year overall survival is greater than 78%

when diagnosed at this early stage [6]. (Table 1) When regional or distant metastases are present at the time of diagnosis, five year survival decreases to 56% and 21%, respectively [6].

Table 1. Staging of endometrial carcinoma (International Federation of Gynecology and Obstetrics [FIGO]) [22] and survival by stage [6].

FIGO stage	Location of Tumor	5-year Overall Survival (%)
IA	Confined to uterus	90
IB	Confined to uterus, >50% myometrial invasion	78
II	Cervical stromal invasion	74
IIIA	Spread to uterine serosa or adnexae	56
IIIB	Vaginal or parametrial involvement	36
IIIC1	Spread to pelvic lymph nodes	57
IIIC2	Spread to para-aortic lymph nodes	49
IVA	Bowel/bladder invasion	22
IVB	Distant metastasis	21

The majority of women with endometrial cancer are cured with surgery alone, and do not require further treatment. The need for adjuvant therapy is based on risk for recurrence, which is stratified by stage, tumor and patient factors. Patients with grade 2 or 3 histology, invasion into the outer third of the myometrium, or lymphovascular space invasion, in combination with increasing age, are designated high-intermediate risk for recurrence by the Gynecologic Oncology Group (GOG) [23]. In this subset of patients, both postoperative pelvic radiation [23] and vaginal brachytherapy have been shown to decrease the rate of recurrence

[24]. Patients with endometrioid histology and stage III or IV disease, or serous and clear cell histology of any stage are defined as having high risk for recurrence, and are typically dispositioned to receive adjuvant therapy. This is a heterogeneous group of patients with rare tumor types, making prospective study challenging. The optimal type of adjuvant therapy has not been defined for either early or advanced stage uterine serous carcinoma, but existing retrospective data suggest that platinum-taxane chemotherapy does improve outcomes, and radiation may decrease local recurrence rates [5,25].

Prognosis is poor in patients who have metastatic or recurrent disease. Approximately 16% of patients with endometrial cancer have regional lymph nodes or widely metastatic spread at the time of diagnosis [26], and 15% of all patients with endometrial cancer eventually develop disease relapse [27], typically within the first three years [27]. Again, this is a heterogeneous group of patients with varying histologies, sites of recurrence, and performance status. Depending on these factors, surgical resection, radiation, chemotherapy, hormonal or targeted therapies may be appropriate [25,26,28,29]. Because of the overall poor prognosis of this group of patients, a better understanding of the biological behavior of these aggressive tumors is warranted.

Genomic characteristics and targeted therapies in endometrial cancer

The Cancer Genome Atlas (TCGA) performed an analysis of 373 endometrial carcinoma samples that provided an in depth view of the genomic characteristics of this disease. The cohort included 307 endometrioid cancer samples and 66 serous or mixed histology samples [30]. Through an integrated genomic and proteomic approach, four tumor subtypes or clusters were identified: ultramutated tumors with frequent POLE mutations and underlying endometrioid histology, hypermutated endometrioid tumors with microsatellite

instability, copy-number low tumors of endometrioid histology, and copy-number high tumors with serous histology. The focus of our work here is primarily on the endometrioid subgroups, which have frequent mutations in PTEN, PIK3CA, CTNNB1, ARID1A, and KRAS. Loss of function of the tumor suppressor gene PTEN is the most common mutation in endometrioid endometrial cancer, and occurs in about 80% of cases [30,31]. PTEN mutations were particularly common in the endometrioid subgroups, which is relevant for our work presented here. These subgroups tend to have infrequent mutations in TP53, however, approximately 25% of the tumors in the TCGA cohort that were classified as high grade (grade 3) endometrioid had molecular characteristics similar to the serous tumors [30]. These characteristics include high frequency of TP53 mutations and somatic copy number alterations, which set them apart from low grade endometrioid tumors. Endometrioid endometrial cancer is thus a diverse disease, and genomic classification may allow providers to offer more individualized care in order to exploit specific molecular characteristics of the tumor.

Microsatellite instability (MSI) occurs in approximately 20% of endometrioid endometrial cancer cases, and results from defects in mismatch repair genes (MLH1, MSH2, MSH6, PMS2) [32]. MSI can occur in the context of Lynch syndrome by means of germline mutations in these genes, which accounts for 2-5% of all endometrial cancer cases [33]. More commonly, microsatellite instability occurs sporadically due to methylation of the MLH-1 promoter. MLH-1 promoter methylation, a form of epigenetic silencing, accounts for approximately 70% of cases of MSI endometrial cancer [3,34]. Bilallelic inactivation of mismatch repair genes, either by mutation or epigenetic silencing, leads to genomic instability via accumulation of DNA mismatches in microsatellite regions [35]. This subtype of endometrial cancer has unique biological behavior as compared to the microsatellite stable,

copy number low endometrioid tumors, and is predictive of a more favorable clinical outcome [36].

The detailed genomic characterization by the TCGA provides a framework for rational therapy in endometrial cancer. Mutations in components of the PI3K/AKT pathway and its targets are common in this disease, and PTEN loss of function, which is frequent, leads to constitutive activation of this pathway [37,38]. The mammalian target of rapamycin (mTOR) is an important downstream target of the PI3K/AKT pathway [39], and the mTOR inhibitors temsirolimus and everolimus have shown activity in patients with advanced or recurrent endometrial cancer [40,41,42]. However, agents individually targeting PI3K and AKT as such have had only modest response rates. Vascular endothelial growth factor (VEGF) expression is associated with increased tumor growth and metastasis in endometrial cancer [43], indicating that bevacizumab, a monoclonal antibody targeting VEGF-A, may be efficacious in this disease. A phase 2 trial of single agent bevacizumab in advanced endometrial cancer yielded promising response rates [44]. Other agents targeting the VEGF pathway, including cediranib and sunitinib, are also under investigation [45]. Despite the variety of rational targets for endometrial cancer therapy, clinical benefit has been modest in recurrent or advanced cases of this disease, emphasizing the need for further investigation.

Homologous recombination deficiency and malignancy

The ability of a cell to survive requires accurate transmission of genetic material to daughter cells, which is dependent on its ability to repair DNA damage prior to cell division [46]. This is accomplished by a complex network of pathways that repair a variety of types of DNA damage, including double strand breaks, which can lead to cellular lethality if improperly repaired [47]. Homologous recombination (HR) is one of the mechanisms by which double

strand breaks, as well as interstrand crosslinks, are detected and repaired. ATM and ATR kinases are early responders to double strand breaks; ATM is recruited to the area of double strand breaks by the Mre11-Rad50-Nbs1 (MRN) complex, an early responder to DNA double strand breaks [48]. ATM phosphorylates several downstream targets which function as tumor suppressors, and their phosphorylation is essential for the initiation of HR. One such downstream target is BRCA1 [49]; upon phosphorylation, BRCA1 localizes to RAD51 foci at sites of double strand breaks during the S and G2 phases of the cell cycle [50,51,52]. The role of BRCA1 in DNA damage repair is diverse [53], and BRCA1 also colocalizes with the MRN complex [54]. BRCA2 plays a similar but distinct role by colocalizing with RAD51 nuclear foci, regulating its activity, and is essential for homology-directed double strand break repair [55,56]. PTEN loss of function has also been implicated in HR deficiency [57] via the inhibition of RAD51 foci formation [58], although its primary role is regulation of the phosphatidylinositol 3-kinase (PI3K)/AKT/mTOR signaling pathway [59,60].

Germline mutations of BRCA1 and 2 are associated with a markedly increased risk of developing breast and ovarian cancer. The population risk varies by study, but when the data from several large studies are considered [61,62,63], in BRCA1 mutation carriers, the lifetime risk of breast cancer is 57-65% and the lifetime risk of ovarian cancer is 40-60%. In BRCA2 mutation carriers, the lifetime risk of breast cancer is 45-47% and the lifetime risk of ovarian cancer is 11-18%. Mutations resulting in nonfunctional BRCA1 or 2 lead to increased sensitivity to inhibitors of poly(ADP-ribose) polymerase (PARP-1), a nuclear protein that is an early responder to DNA single strand breaks along the base excision repair pathway and prevents further processing of DNA until breaks are repaired [64]. The loss of PARP-1 function inhibits repair of single strand breaks, which in turn increases the quantity of DNA lesions to be repaired by HR in the S phase [65]. In cells lacking BRCA1 or 2 function, and thus deficient in HR, the inhibition of PARP-1 results in chromosomal instability, cell cycle arrest and

eventual cell death [66,67]. Likewise, in some preclinical studies as well as a case report, loss of PTEN function showed increased sensitivity to PARP inhibition [58,68]. The use of PARP inhibitors has proven to be an effective strategy in patients with breast [69] and ovarian cancer [70] and germline BRCA1 or BRCA2 mutations. Indeed, olaparib, an oral inhibitor of PARP, was approved by the FDA in 2014 for use in patients with recurrent ovarian cancer and a BRCA mutation. In a phase 2 trial of olaparib maintenance therapy in patients with relapsed ovarian cancer [71], patients with BRCA mutations derived the greatest survival benefit from the use of olaparib as maintenance therapy. However, patients with wild type BRCA treated with olaparib also had significantly longer progression free survival than those treated with placebo, suggesting other mechanisms for susceptibility to PARP inhibition may be involved, including mutations in other genes important for HR [72].

The homologous recombination deficiency (HRD) score

Genomic instability secondary to homologous recombination deficiency (HRD) can be caused by a multitude of genetic aberrations and has many important contributors besides BRCA deficiency. Recently, techniques have been developed that allow investigators to capture and understand the degree of HRD in a tumor. Three independent DNA-based metrics have been developed to detect major contributors to genomic instability due to HRD: loss of heterozygosity (HRD-LOH score) [73], telomeric allelic imbalance (HRD-TAI score) [74], and large-scale state transition (HRD-LST score) [75]. The HRD-LOH score refers to the number of regions of LOH in the tumor longer than 15Mb but shorter than the whole chromosome [73]. The HRD-TAI score is the number of regions in the tumor with allelic imbalance that extend to one of the subtelomeres but do not cross the centromere [74]. HRD-LST identifies chromosome breaks including inversions, translocations and deletions in adjacent segments of at least 10Mb, and the score is equal to the number of break points between regions [75].

All three metrics are associated with platinum sensitivity in breast and ovarian cancer, and correlate with mutations in BRCA1 and 2 as well as other HR pathway genes [76]. While each has clinical relevance separately, the sum of the three metrics (HRD-LOH, HRD-TAI, HRD-LST), known as the HRD score, is a more robust predictor of HR deficiency than each score alone in breast and ovarian cancer patients [76,77]. In addition, HRD score is a better predictor of platinum sensitivity than clinical variables or BRCA mutation status; indeed, when wild type BRCA tumors were analyzed, platinum response was superior in patients with high HRD scores [77].

The clinical implications of HR deficiency in breast and ovarian cancer due to BRCA mutation status are well-established, and new information about HR deficiency due to other causes continues to emerge. There is limited knowledge, however, about the clinical significance of HR deficiency in endometrial cancer. Preclinical work and genomic analysis by TCGA suggests that HR deficiency may be an important factor in the biological behavior of these tumors. Because of the high prevalence of this disease, and the paucity of effective treatments in advanced cases, further investigation is certainly warranted.

Hypothesis and specific aims

Hypothesis: In patients with endometrial cancer, defects in the homologous recombination pathway will be associated with worse clinical outcomes, and homologous recombination deficiency (HRD) score will be both predictive and prognostic in this disease.

Specific aim 1: Determine the frequency and clinical significance of homologous recombination pathway alterations in endometrial cancer.

Specific aim 2: Assess the effect of HRD on tumor growth and response to PARP inhibition in murine orthotopic models of uterine cancer.

Materials and Methods

Cell line maintenance

Endometrial cancer cell lines (AN3CA, Hec1a, Hec1b, Hec265, Ishikawa, and KLE) were obtained from the American Type Culture Collection. All cell lines were maintained in 5% CO_2 at 37 °C. Hec265 cells were maintained and propagated in RPMI 1640 (GE Healthcare Life Sciences) supplemented with 15% fetal bovine serum and 0.1% gentamicin sulfate (GeminiBioproducts). Ishikawa cells were maintained and propagated in MEM (Mediatech, Inc) supplemented with 10% fetal bovine serum and 0.1% gentamicin sulfate. Hec1a cells were maintained and propagated in McCoy's 5A medium (Mediatech, Inc) supplemented with 10% fetal bovine serum and 0.1% gentamicin sulfate. Hec1b and AN3CA cells were maintained in MEM supplemented with 10% fetal bovine serum, glutamine, sodium pyruvate (Lonza BioWhittaker) and non-essential amino acids (Life Technologies Laboratories). KLE cells were maintained and propagated in 1:1 DMEM:F12 media (Sigma-Aldrich) supplemented with 10% fetal bovine serum and 0.1% gentamicin sulfate[78].

Cell lines were obtained within one year of the work described, and per institutional policy (MD Anderson policy ACA#1044) cell line authentication was performed at least once per year. Authentication was performed by the short tandem repeat method using the Promega Power Plex 16HS kit (Promega). Somatic mutations were detected using a Sequenom MALDI TOF MassArray system (Sequenom). Mycoplasma detection was performed using the MycoAlert Kit (Lonza), and all experiments were conducted with 60-80% confluent cultures[78].

siRNA transfections

Hec1a was selected for use *in* vivo and all transfections were performed using this cell line. All siRNA transfections were performed using Lipofectamine 2000 (Invitrogen) reagent using forward transfection protocol from the manufacturer. Cells were seeded in 6 well plates at low density, and media was changed six hours after transfection to minimize toxicity. The siRNA sequences used for BRCA1 siRNA experiments are as follows: Control: Sense UUCUCCGAACGUGUCACGU / Antisense ACGUGACACGUUCGGAGAA, sequence #1: Sense CUACUGUCCUGGCUACUAA / Antisense UUAGUAGCCAGGACAGUAG (Sigma-Aldrich, SASI_Hs01_00179500), sequence #2: Sense CUAUGCAAGGGUCCCUUAA / Antisense UUAAGGGACCCUUGCAUAG (Sigma-Aldrich, SASI_Hs01_00179502). Following forward transfection, cells were incubated for 48, 72 or 96 hours. Trizol reagent (Invitrogen) was then added to cells in preparation for RNA isolation[79].

Quantitative real-time PCR

For mRNA quantification, total RNA was isolated using the Qiagen RNeasy kit (Qiagen). Using 1,000 ng of RNA, complementary DNA was synthesized using a Verso cDNA kit (Thermo Scientific), as per the manufacturer's instructions. Analysis of mRNA levels was performed on a 7500 Fast Real-Time PCR System (Applied Biosystems, CA) with SYBR Green-based real-time PCR for all genes. PCR was done with reverse-transcribed RNA and 100 ng/µL of sense and antisense primers in a total volume of 20 µL. Each cycle consisted of 15 seconds of denaturation at 95°C and 1 minute of annealing and extension at 60°C (40 cycles)[79]. BRCA1 primer sequences, Forward: 5' TGTGAAGGCCCTTTCTTCTG, Reverse: 5' TCCCATCTGTCTGGAGTTGA. 18S was used as a housekeeping gene; primer sequences, Forward: 5' CGCCGCTAGAGGTGAAATTC, Reverse: 5' TTGGCAAATGCTTTCGCTC.

Liposomal nanoparticle preparation

BRCA1 sequence #2 was selected for *in vivo* use based on knockdown efficiency as determined by quantitative real-time PCR. siRNA for *in vivo* delivery was incorporated into DOPC nanoliposomes [80,81,82]. DOPC and siRNA were mixed in the presence of excess tertiary butanol at a ratio of 1:10 (w/w) siRNA/DOPC. Tween 20 was added to the mixture in a ratio of 1:19 Tween 20: siRNA/DOPC. The mixture was vortexed, frozen in an acetone/dry ice bath, and lyophilized. Before in vivo administration, this preparation was hydrated with PBS at room temperature at 5 µg in 200 µl of PBS per injection[83]. Treatment was given twice weekly via intraperitoneal injection.

In vivo models

Female athymic nude mice were purchased from Taconic Farms (Hudson, NY). Mice were housed and cared for according to guidelines set forth by the American Association for Accreditation of Laboratory Animal Care and the US Public Health Service policy on Human Care and Use of Laboratory Animals. All mouse studies were approved and supervised by The University of Texas MD Anderson Cancer Center Institutional Animal Care and Use Committee. All animals were 8–12 weeks old at the time of cell injection.

Prior to injection into mice, cells were harvested using trypsin-EDTA (GE Healthcare Life Sciences), neutralized with complete media, washed and resuspended in Hanks' balanced salt solution (HBSS; Gibco). Cells were injected into the left uterine horn (4×10^6 cells in 100 µl of HBSS). Prior to injection, mice were anaesthetized with a combination of ketamine (100mg/kg), xylazine (2.5mg/kg) and acepromazine (2.5mg/kg), given intraperitoneally in a volume of 200 µl. To inject cells, an incision in the midline was made and using blunt dissection, the left uterine horn identified. A 1-ml tuberculin syringe with a 30-gauge needle was used to inject the cell suspension directly into the uterine horn. After

injection, the incision was closed using interrupted 4-0 Vicryl sutures followed by surgical clips and the mouse was returned to a warmed cage until fully recovered. Mice received buprenorphine for analgesia at the time of surgery and twice daily for 72 hours postoperatively.

For all therapeutic experiments, Olaparib (LC Laboratories) was administered at a dose of 50mg/kg by oral gavage daily. Olaparib was dissolved in DMSO and then diluted 10% v/v in 2-hydroxy-propyl-β-cyclodextrin (Sigma-Alridch) [84,85,86]. siRNA was given intraperitoneally twice weekly. Treatment with siRNA began 10 days after cell injection and treatment with olaparib began 14 days after cell injection, and continued for approximately three to four weeks. Once mice in any group became moribund, all mice were sacrificed and necropsied. Tumors were harvested, and weight, number and location of metastatic nodules were recorded. Tumor tissue was preserved and fixed in formalin for paraffin embedding, frozen in optimal cutting temperature media to prepare frozen slides, or snap-frozen for lysate preparation.

Immunoblotting

Lysates from cultured cells were prepared using modified RIPA buffer (50 mM Tris–HCl [pH 7.4], 150 mM NaCl, 1% Triton, 0.5% deoxycholate) plus 25 μg ml^{-1} leupeptin, 10 μg ml^{-1} aprotinin, 2 mM EDTA and 1 mM sodium orthovandate. The protein concentrations were determined using a BCA Protein Assay Reagent kit (Pierce Biotechnology). Lysates were loaded and separated on SDS–PAGE. Proteins were transferred to a nitrocellulose membrane by semidry electrophoresis (Bio-Rad Laboratories) overnight, blocked with 5% milk for one hour and then incubated at 4°C overnight with primary antibody: BRCA1 (Santa Cruz Biotechnology, sc-642 [1:500]), RAD51 (Santa Cruz Biotechnology, sc-8349 [1:500]), p-H2AX (Cell Signaling, 9718P [1:1000]). After washing with tris-buffered saline with Tween 20, membranes were then incubated with horseradish peroxidase-conjugated horse anti-Mouse

(GE Healthcare, NA931V [1:2000]) or Rabbit (GE Healthcare, NA934V [1:2000]) IgG for one hour. Visualization of horseradish peroxidase was performed using an enhanced chemiluminescence detection kit (Pierce Biotechnology). To confirm equal sample loading, the blots were probed with an antibody specific for vinculin (Sigma-Aldrich, V9131 [1:5000]).[78]

Cell viability assays

MTT: Cell viability assays were performed by testing cell's ability to reduce the tetrazolium salt [3-(4,5-dimethylthiazol-2-yl)-5-(3-carboxymethoxyphenyl)-2-(4-sulfophenyl)-2H-tetrazolium, inner salt] to a formazan. Cells were seeded in a 96-well plate at low density. 24 hours after seeding, cells were treated for 72 hours with increasing concentrations of paclitaxel, for 96 hours with increasing concentrations of cisplatin, or for 7 days with increasing concentrations of olaparib. After the designated time based on treatment, cells were incubated with 0.15% 3-(4,5-dimethylthiazol-2-yl)-2,5-diphenyltetrazolium bromide (MTT) for 2 hours at 37°C. The supernatant was removed, cells were dissolved in 100-µL DMSO, and the absorbance at 540 nm was recorded[78].

Colony formation assay: Cells were seeded in 6-well plates at low density. 24 hours after seeding, cells were treated with increasing concentrations of paclitaxel, cisplatin or olaparib for 72, 96 hours or 7 days, respectively. Following treatment, colonies were stained with a solution of 0.25% crystal violet and 50% methanol in PBS. Colonies containing 50 or more cells were counted manually using ImageJ software.

Immunohistochemistry and immunofluorescence

Paraffin-embedded tissues were used to detect cell proliferation (with Ki67) and apoptosis (with cleaved caspase 3). Sections were deparaffinized sequentially in xylene and

declining grades of ethanol prior to rehydration and transferred to PBS. After antigen retrieval with citrate buffer (pH 6.0), the sections were blocked with 3% hydrogen peroxide in methanol and protein blocker at room temperature. The sections were then incubated with the Ki-67 (DakoCytomation [1:200]) or monoclonal mouse antibody against cleaved caspase 3 (Biocare Medical [1:100]) overnight at 4°C. After being washed with PBS, sections were incubated with horseradish peroxidase-conjugated rat anti-mouse immunoglobulin G2a (Serotec, Harlan Bioproducts for Science [1:100] for Ki67 staining) for 1 hour, or biotinylated 4+ goat anti-rabbit secondary antibody (Biocare Medical) for 20 minutes followed by streptavidin 4+ (Biocare Medical) for 20 minutes for cleaved caspase 3 staining. To quantify Ki67 expression and cleaved caspase 3, five samples from each group were examined. The number of positive cells was determined in five random fields at 40x magnification.

γ-H2AX staining was performed on frozen sections. Sections were fixed in cold acetone for 15 min and washed with PBS. Immunofluorescent staining was performed using phospho-histone H2AX antibody (Cell Signaling, 9718S, 1:500), according to the manufacturer protocol. Slides were developed with 3, 3”-diaminobenzidine chromogen (Invitrogen, Carlsbad, CA) and counterstained with Gil’s No. 3 hematoxylin (Sigma-Aldrich). The number of γ-H2AX foci per cell was determined in five random fields at 40x magnification.

Patient tumor samples

After the study was approved by the Institutional Review Board and written informed consent was obtained from the patients for the use of clinical specimens for research, 156 formalin-fixed paraffin-embedded (FFPE) endometrioid endometrial adenocarcinoma tumor samples were obtained from the MD Anderson Cancer Center Tumor Bank. Demographic,

clinical and outcome data were obtained from patient records. Responses to initial treatment and treatment for recurrent disease were recorded.

HRD score calculation

For each patient, one 5-micron slide and five 10-micron slides cut from FFPE primary endometrial tumor specimens were sent to Myriad Genetics, Inc (Salt Lake City, UT). All tissue was processed in the research laboratory according to the CLIA protocol. A 5-micron hematoxylin and eosin slide was created and reviewed by the pathologist to facilitate enrichment of tumor-derived DNA. DNA extraction was performed on 10-micron sections in the area of highest tumor cell density [77]. DNA was analyzed using a next-generation sequencing-based assay to generate a genome-wide single nucleotide polymorphism (SNP) profile from which the three components of the HRD score are calculated. The panel used targets 54,091 SNPs distributed across the genome. A detailed description of the assay is available in Timms, et al [76].

MSI assay

35 microsatellites which could be used to measure MSI were identified within the SNP flanking sequence from the HRD assay. The criteria for these microsatellites were 1) the microsatellite was within 100 based of the SNP position, 2) the microsatellite was 15-20 bases in length, 3) the average SNP coverage was over 100 independent reads, 4) the microsatellite was of a consistent length among normal tissue samples with low noise around the defaults length having CV less than 20%, and 5) in a control set of MSI positive samples two or more samples must exhibit instability around the same microsatellite. The length of all 35

microsatellites is assessed in all samples. If ≥3 microsatellites show deletions then the sample is defined as MSI positive.

High mutation load (HML) assay

Somatic mutation load is assessed by analysis of SNP flanking sequence from the HRD assay. The forward and reverse read sequenced, trimmed for quality, were aligned to 801 bp segments around each target SNP, with a maximum of 7 mismatches and no gaps used as criteria to exclude low quality reads. Mismatches between the template segment sequences and the read sequences were counted for each test locus. Excluded from the analysis were repetitive positions, positions with SNPs listed by NCBI's dbSNP, positions with consistently low coverage among different samples (with coverage <50 in half of more of 100 previously tested samples), and positions that were found by previous analysis to consistently have mutations in unrelated samples (mutated in more than one sample out of 100 previo usly tested samples). The remaining 9,084,648 test loci were used to count mutations. Analysis was limited to bases with a minimum of 50 independent reads, and only independent reads were included in the analysis. The analysis was limited to variants with allele rations in the range 11%-65%. Samples were considered to have high mutation load if they exhibited greater than 50 test loci harboring variants.

Analysis of data from TCGA

Level 1 TCGA exome sequencing data for 499 uterine corpus endometrial carcinoma (UCEC) tumor-normal pairs were downloaded from the Cancer Genomics Hub. VarScan2 was used to make somatic mutation calls, including both single nucleotide polymorphisms and insertion-deletions. ANNOVAR was used to annotate the mutation points and extract the

exonic alterations, including synonymous single nucleotide variants (SNV), non-synonymous SNV, stop gain SNV, non-frameshift insertions, non-frameshift deletions, frameshift insertions and frame shift deletions. Samples with non-synonymous SNV, stop gain SNV or insertions-deletions in a gene were defined as having mutations in that specific gene. For samples with more than one mutation site, insertions-deletions were considered to be the most severe category, followed by stop gain SNV, non-synonymous SNV, and synonymous SNV; each sample was assigned to the most severe category matched.

Statistical analysis

Continuous variables were compared with the two-sample t test (between two groups) or with one-way analysis of variance (ANOVA; for all groups) if normally distributed (as determined by the Kolmogrov-Smirnov test), and the Mann-Whitney test was used if distributions were nonparametric. A *p*-value of less than 0.05 from a two-tailed statistical test was considered statistically significant. All statistical tests were two-sided[87]. All p-values appearing on Kaplan-Meier curves are two-sided p-values from log-rank tests. HRD scores are grouped into non-continuous categories.

Results

Homologous recombination pathway alterations in endometrial cancer

Analysis of TCGA data

To determine the frequency and clinical significance of alterations in homologous recombination pathway genes in endometrial cancer, TCGA data were queried. Data for 499 patients with endometrial cancer were analyzed. Of these, 76 patients (15%) had serous

histology, 335 (67%) had endometrioid histology, 18 (4%) had mixed histology, and in the remaining 70 patients (15%), histology was unknown. First, emphasis was placed on somatic mutations in BRCA, due to the established role of germline BRCA mutations in breast and ovarian cancer. In addition, TCGA was queried to determine the frequency and clinical significance of somatic PTEN mutations in in this cohort, as it is frequently mutated in endometrial cancer and some preclinical studies support the role of PTEN in HR deficiency. In the TCGA cohort, mutations in BRCA1 or 2 were present in 52 of the 335 patients (16%) with endometrioid histology. PTEN mutations were present in 260 of 335 patients (78%), and presented with a concomitant BRCA1 or 2 mutation in 47 patients (14%). (Figure 1)

Figure 1. Mutations in BRCA1, BRCA2 and PTEN in the TCGA endometrioid cohort (N=335)

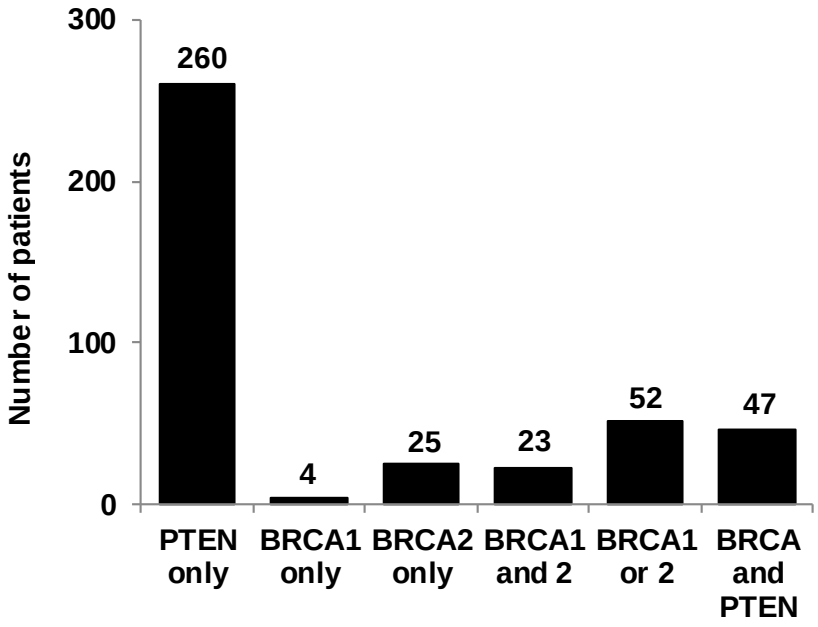

In the subset of 52 patients who had BRCA mutations, 34 (65%) had stage I disease and the remainder had stage II disease or higher. (Table 2)

Table 2. Distribution of BRCA mutations by stage in the TCGA endometrioid cohort (N=335)

Stage	Number of patients (%)
I	34 (64)
II	6 (12)
III	10 (20)
IV	2 (4)

When BRCA and PTEN somatic mutations were examined in relation to overall survival in the TCGA cohort, which included endometrioid, serous and mixed histologies, patients with concomitant BRCA and PTEN somatic mutations had significantly improved survival as compared to patients who were wild type for both genes (p=0.02). (Figure 2)

Figure 2. Kaplan-Meier plot of overall survival in the entire TCGA cohort (N=499)

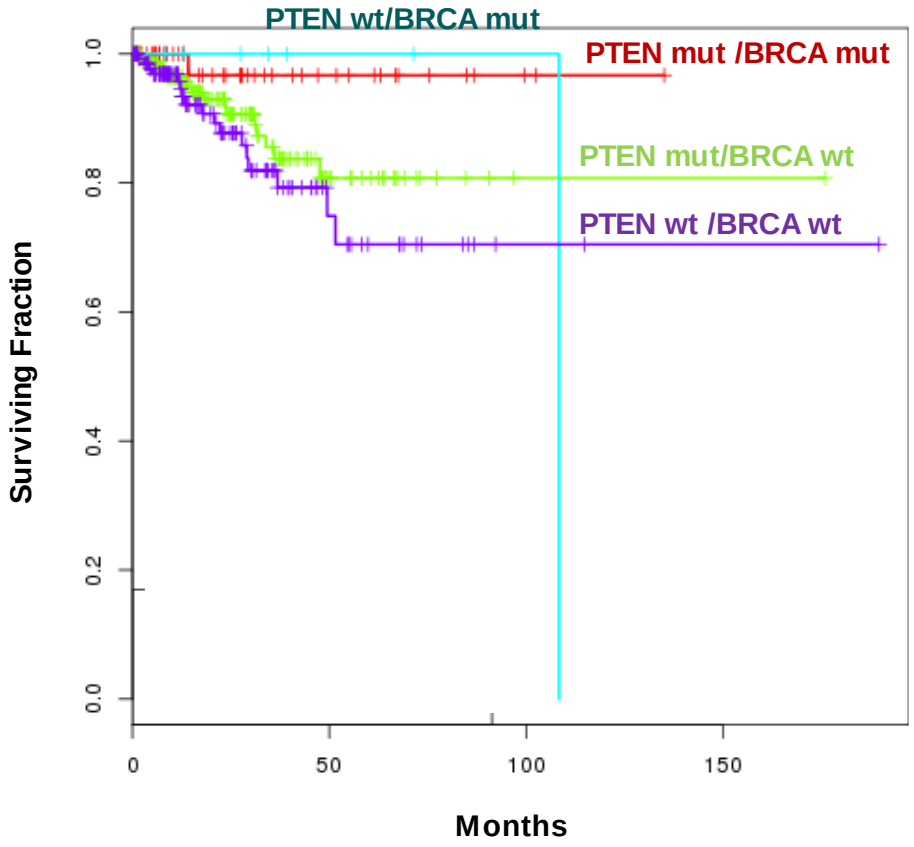

When BRCA and PTEN somatic mutations were examined in relation to overall survival in the endometrioid portion of the TCGA cohort (N=335), there was no significant difference in survival when patients with both BRCA and PTEN mutations were compared to patients who were wild type for both genes (p=0.18). (Figure 3)

Figure 3. Kaplan-Meier plot of overall survival in the TCGA cohort, endometrioid histology only (N=335)

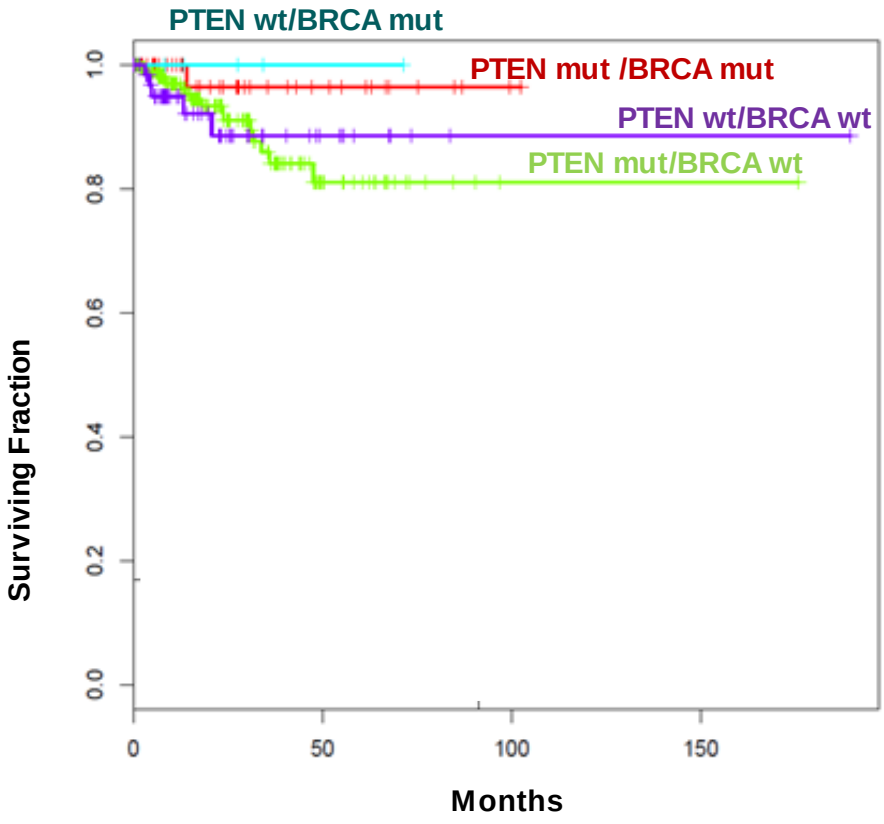

Given that there was a significant difference in survival within the entire cohort when BRCA/PTEN double mutants were compared with those who were wild type for both genes, and this survival difference was not present when the endometrioid histology was examined alone, we postulated that the patients with serous or mixed subtypes may be driving the survival difference seen when the entire cohort was examined together. When the patients with serous and mixed histology tumors were examined alone, there was no significant difference in survival between BRCA/PTEN double mutants and those who were wild type for both genes (P=0.37). It is likely that within the serous and mixed group, the number of patients with BRCA and PTEN mutations was not large enough to detect differences in survival.

Analysis of MD Anderson patient data

To address the higher than expected frequency of BRCA mutations in the TCGA cohort, and to address the possible role of HR deficiency in endometrial cancer, we utilized a cohort of patients enriched for endometrioid histology and whom had received adjuvant therapy of any kind. Because the majority of patients with endometrioid endometrial cancer are cured by surgery alone and do not require adjuvant therapy, we chose to focus on those with advanced stage and high-intermediate risk features as these are the patients that would most likely benefit from targeted therapy. The cohort included 156 patients. Patient median age at diagnosis was 62 years. 54% of patients presented with stage I disease, 11% presented with stage II disease, 27% presented with stage III disease, and 8% presented with stage IV disease. 1% of patients had FIGO grade 1 histology, 73% of patients had grade 2 histology, and the remaining 26% had grade 3 histology. 74 of 156 patients (47%) received platinum chemotherapy, and the remaining 82 (53%) received radiation only (by any route). All 156 samples were submitted to Myriad Genetics for processing. Of the 156 patient samples submitted, 137 samples had adequate tissue for laboratory processing. Of these 137 samples,

HRD score was determined for 112 samples and MSI status was determined for 126 samples; the remainder of the samples failed the analysis. HML status was determined for all 137 samples. All three molecular tests were determined on 104 samples. The median HRD score was 3, with a range of 0 to 54 (Figure 4). The data set is skewed right and has a mean HRD score of 5.5.

Figure 4. Histogram of HRD scores in MD Anderson patient cohort.

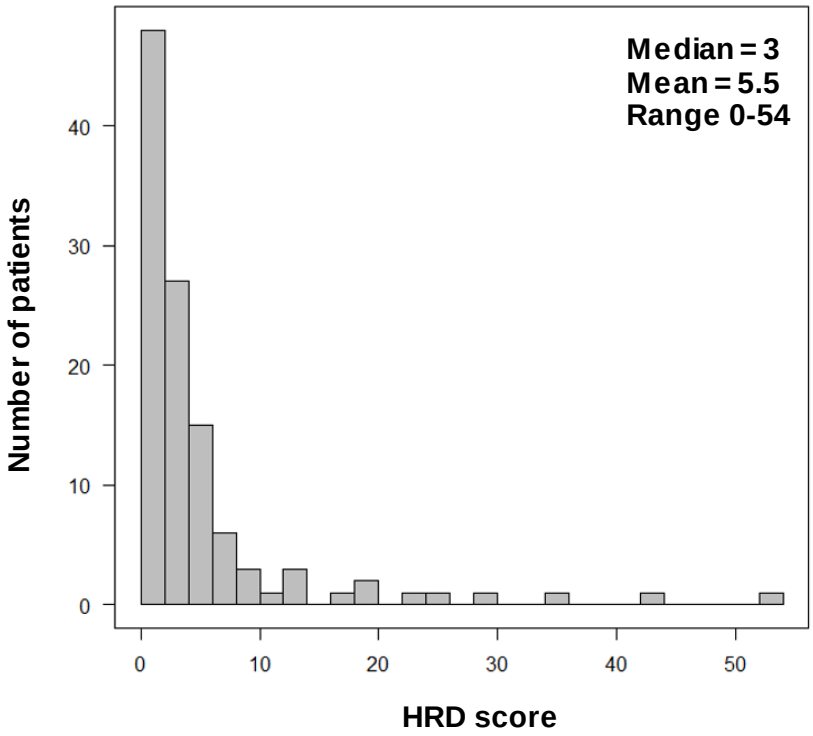

When the cohort is divided into two groups, scores greater than or equal to 10 and scores less than 10, there is no significant difference in survival between the groups (P=0.17). (Figure 5) An HRD score of 10 was chosen as a cut off because the majority of tumors in our cohort

with somatic mutations in TP53 have scores of 10 or greater, and the majority of the oncogene mutated tumors, as well as MSI and HML positive tumors have scores less than 10. The differences in mutational profiles are thought to contribute to biological differences in the tumors. While there was no statistically significant difference between the groups, the patients with higher HRD scores trended toward worse survival. Initially, the cohort was split at the median of 3 to divide the cohort into high and low HRD score groups and there was a statistically significant survival difference between the two groups (P=0.003), favoring those with low HRD scores. However, due to the fact that many of the patients in our cohort had very low HRD scores (Figure 4), this was not felt to be a clinically significant cutoff between patients who had HR deficiency and those who did not. Using an HRD score of 10 reflects their differing mutational profiles and is likely to be more clinically relevant.

Figure 5. Kaplan-Meier plot of disease free survival, HRD score ≥ 10 vs HRD score < 10.

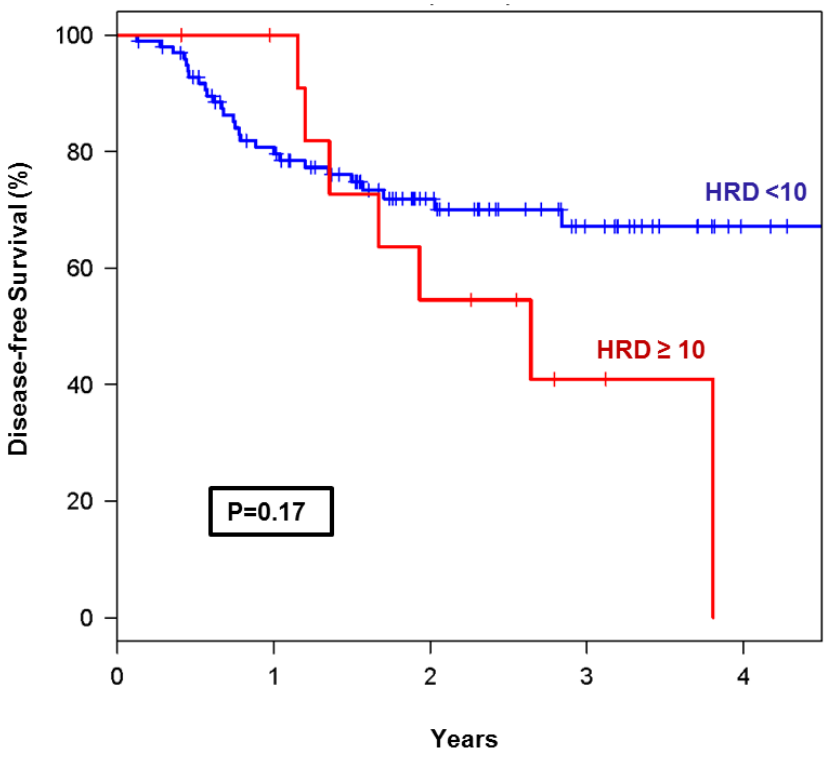

When testing for microsatellite instability was performed on tumor samples and the patients with MSI (N=36) were compared to those who had microsatellite stable tumors (N=90), there was no statistically significant difference in survival between groups (P=0.53). (Figure 6)

Figure 6. Kaplan-Meier plot of disease free survival, MSI-positive vs MSI-negative tumors.

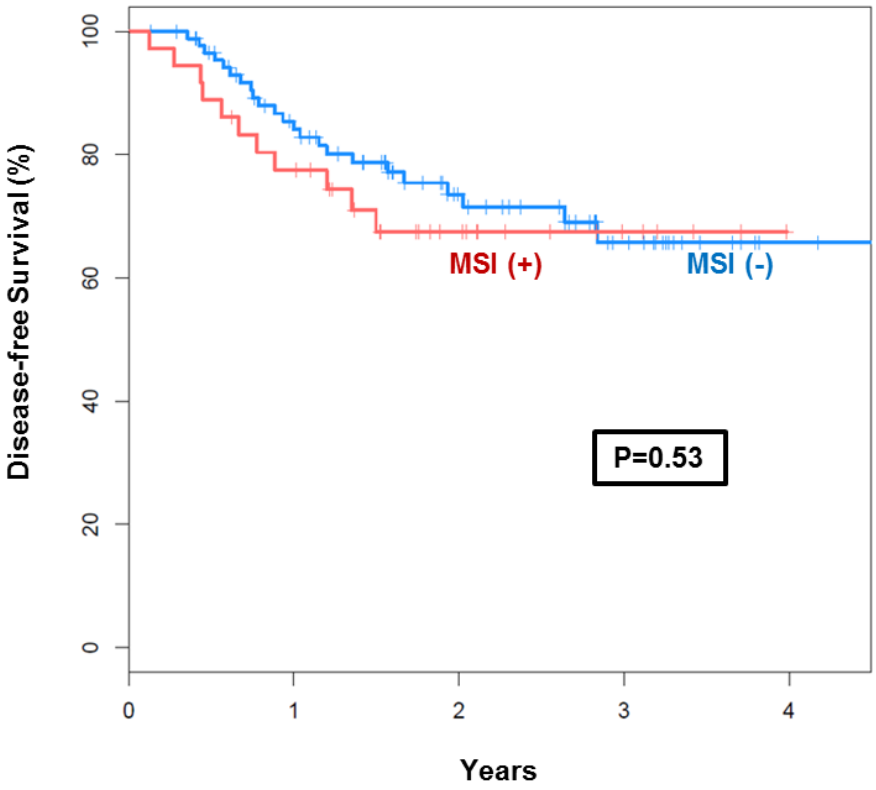

Testing for high mutation load (HML) was also performed. When patients with HML positive tumors (N=12) were compared with HML negative tumors (N=125), there was no significant difference in survival between the groups (P=0.15). (Figure 7)

Figure 7. Kaplan-Meier plot of disease free survival, HML-positive vs HML-negative tumors.

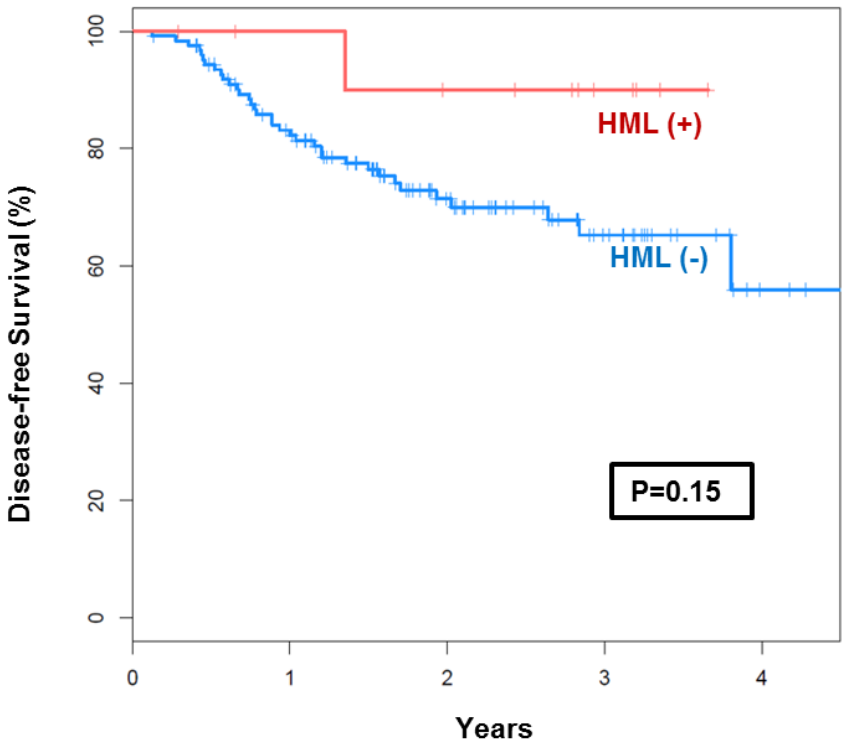

The cohort was then separated into four groups according to molecular subtype: 1. Tumors with high mutation load (HML positive; MSI negative; any HRD status): 8 patients, 2. Tumors with MSI (MSI positive; HML negative; any HRD status): 36 patients, 3. Tumors with HRD score greater than or equal to 10 (MSI and HML negative): 10 patients, and 4. All others: 56 patients. Groups 1-3 had HRD scores less than 10. These analyses were based on 110

patients, which includes the 104 patients with passing results for all three molecular scores, plus 6 patients who failed HRD scores but met criteria to be included in the HML positive or MSI positive groups. There was no significant difference in survival between the four groups (p=0.13), however, the patients with HRD scores above 10 tended to have worse outcomes (Figure 8)

Figure 8. Kaplan-Meier plot of disease free survival in relation to HRD score, MSI and HML status for the entire MD Anderson cohort.

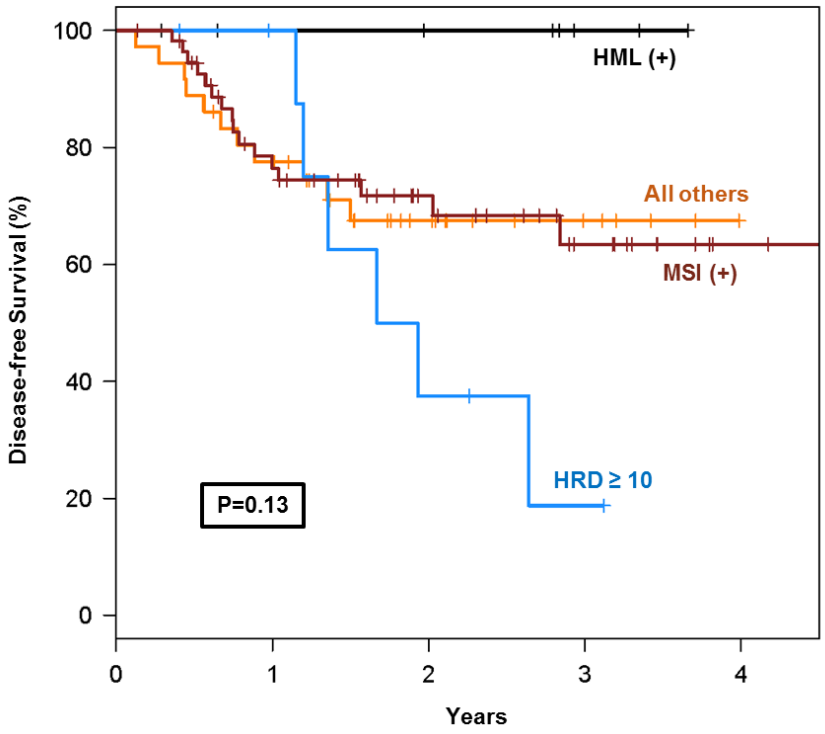

The cohort was then split into two groups: the patients with stage I and II disease (N=67), and the patients with stage III and IV disease (N=43). When the analysis was performed on these two groups (Figure 9 and Figure 10), the trend survival trends remained the same (P=0.31 and P=0.52, respectively). Patients with HRD scores ≥ 10 were found in all disease stages.

Figure 9. Kaplan-Meier plot of disease free survival in relation to HRD score, MSI and HML status for the stage I and II patients in the MD Anderson cohort.

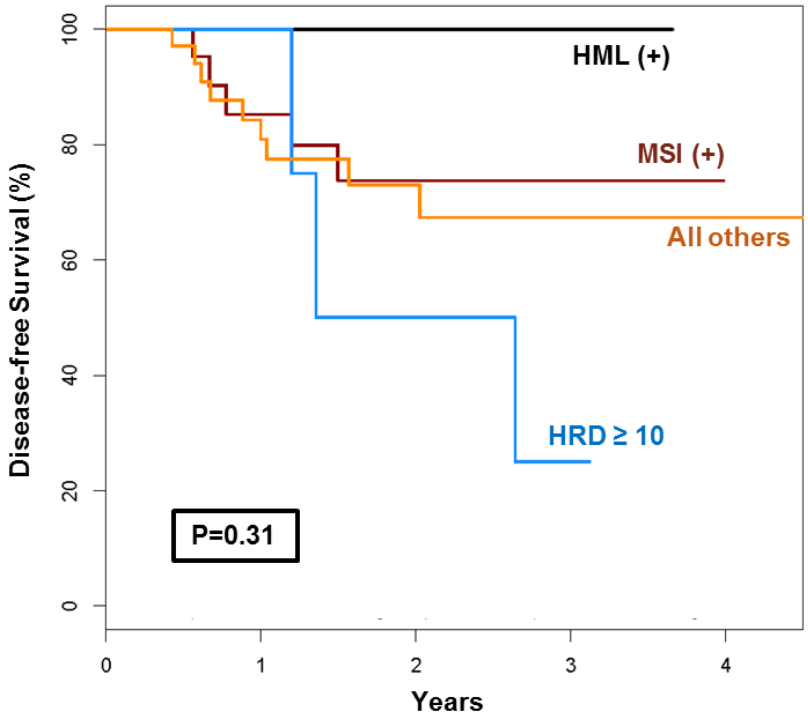

Figure 10. Kaplan-Meier plot of disease free survival in relation to HRD score, MSI and HML status for the stage III and IV patients in the MD Anderson cohort.

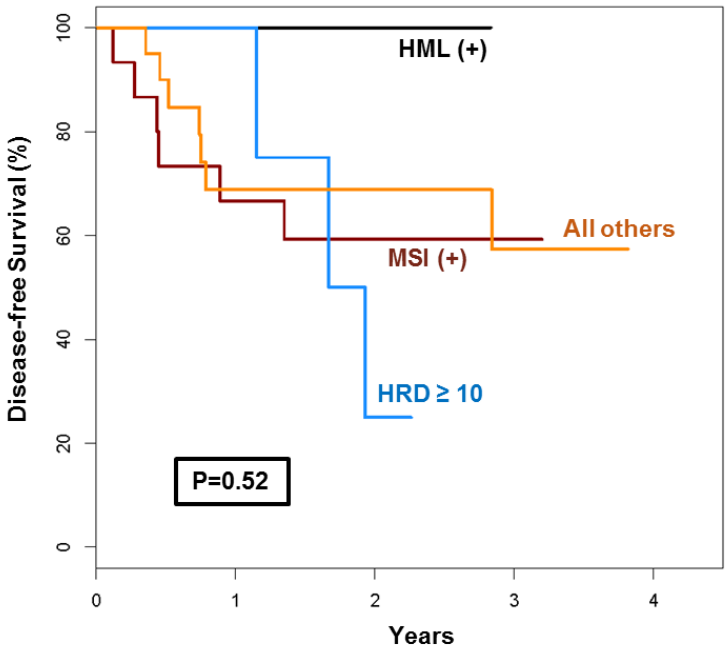

Overall, while there is not a significant difference in survival at the 5% level between the groups, dividing the groups as such by molecular subtype provides a clinically relevant means of capturing survival differences between tumors that are HR deficient and those that are not.

Effect of HRD on tumor growth

HRD score has been shown to be a better predictor of platinum sensitivity than BRCA mutation status in breast cancer patients [77], so we performed a series of experiments to determine whether HRD score had a similar predictive ability in endometrial cancer. First, the HRD score of a panel of endometrial cancer cell lines were assessed. Cell viability after treatment with cisplatin, paclitaxel and olaparib was determined and the cell lines were categorized as either sensitive or resistant to each agent. Platinum-taxane combination

therapy is often used in advanced endometrial cancer and was therefore selected for *in vitro* use. Olaparib was selected for *in vitro* and *in vivo* use due to its known efficacy in the setting of HR deficiency due to BRCA mutation. Finally, an *in vivo* experiment was performed in which mice were injected with tumor cells, and treated with siRNA targeting BRCA1, or a control sequence. Within each group, half of the mice were treated with olaparib, with the goal of determining whether functional BRCA was necessary for response to olaparib. BRCA1 was selected as a target due to its diverse role in HR and significant contribution to hereditary ovarian cancer. We hypothesized that in a high HRD score cell line, olaparib treatment would lead to decreased tumor growth, regardless of whether BRCA1 was functional or not.

Characterization of endometrial cancer cell lines

HRD scores were determined for 12 established endometrial cancer cell lines (Figure 11) using the same method as described above for the patient samples. HRD scores ranged from 2 to 24. A panel of six cell lines with varying HRD scores were selected for experimental use from those listed in Figure 11: Ishikawa (HRD score 6), AN3CA (HRD score 11), Hec265 (HRD score 12), Hec1a (HRD score 19), KLE (HRD score 20) and Hec1b (HRD score 24). Table 3 demonstrates the BRCA1, BRCA2 and PTEN mutation status as obtained from the Cancer Cell Line Encyclopedia, as well as HRD score, of the six selected cell lines. The three cell lines with highest HRD scores (Hec1a, Hec1b, KLE) are wild type BRCA1, BRCA2 and PTEN.

Figure 11. HRD scores of endometrial cancer cell lines.

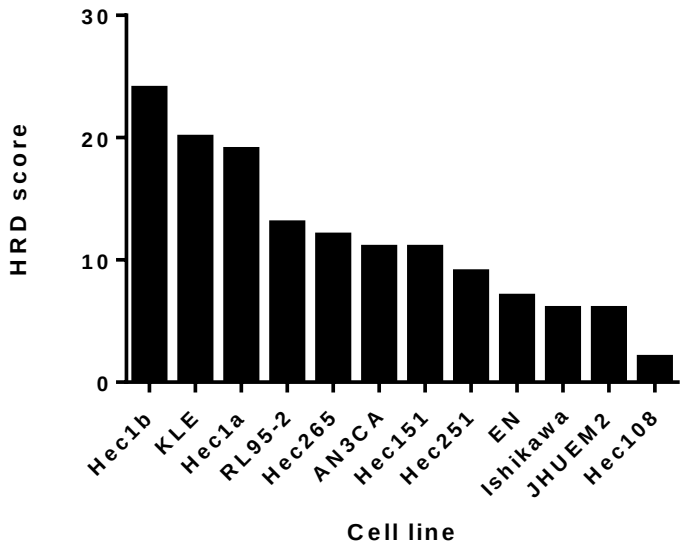

Table 3. BRCA1, BRCA2 and PTEN mutation status and HRD scores of selected endometrial cancer cell lines.

	BRCA1	BRCA2	PTEN	HRD Score
AN3CA	WT	WT	Mut	11
Hec265	Mut	WT	Mut	12
Ishikawa	Mut	WT	Mut	6
KLE	WT	WT	WT	20
Hec1a	WT	WT	WT	19
Hec1b	WT	WT	WT	24

Identification of sensitive and resistant cell lines

In order to determine the sensitivity of the selected cell lines to cisplatin, paclitaxel and olaparib, MTT and colony formation assays were performed with each drug. Advanced endometrial cancer is often treated with platinum-taxane combination chemotherapy, so these were selected for *in* vitro use. Olaparib was selected based on its known efficacy in patients with BRCA mutations. MTT and colony formation assay were performed after treatment with cisplatin for 96 hours (Figure 12). Half maximal inhibitory concentration (IC50) represented in the figures below was then determined for each cell line by averaging the IC50 obtained from the MTT and colony formation assays, which were repeated in triplicate. Error bars for the figures below represent the standard error of the mean. IC50 values ranged from 2.05µM to 23.14µM after treatment with cisplatin. Hec1b was the most sensitive cell line with IC50 3.46 µM, and Ishikawa was the most resistant with IC50 22.2 µM.

Figure 12. Effect of cisplatin treatment on endometrial cancer cell lines. Red: resistant, blue: sensitive.

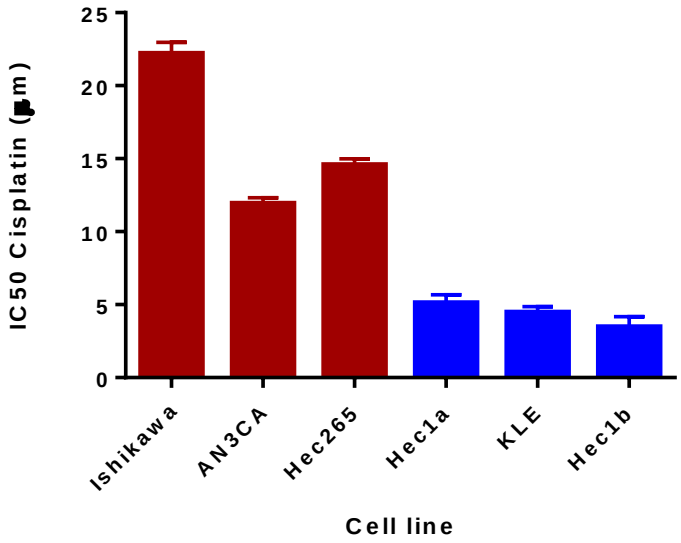

MTT and colony formation assay were performed after treatment with olaparib for 7 days (Figure 13). IC50 was determined for each cell line, and IC50 values ranged from 10.7μM to 223.43μM. Hec1a was the most sensitive cell line with IC50 11.8 μM, and Ishikawa was the most resistant with IC50 209.5 μM.

Figure 13. Effect of olaparib treatment on endometrial cancer cell lines. Red: resistant, blue: sensitive.

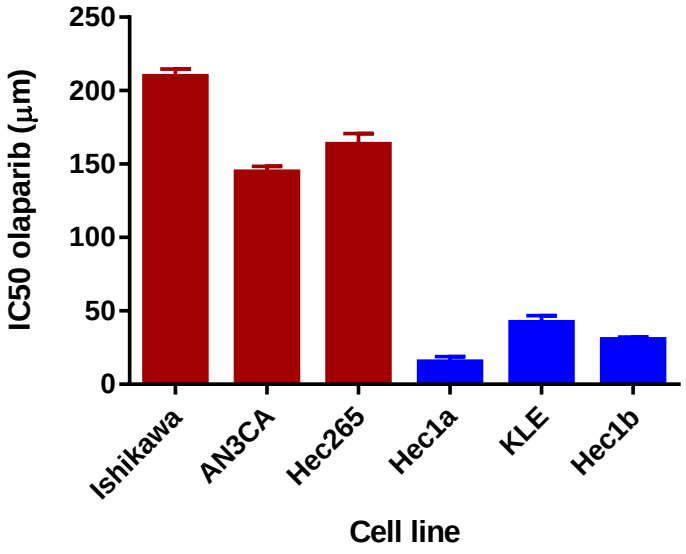

MTT and colony formation assay were performed after treatment with paclitaxel for 72 hours (Figure 14). IC50 was determined for each cell line, and the IC50 values ranged from 3.22µM to 365.90µM. KLE was the most sensitive cell line with IC50 4.86 µM, and AN3CA was the most sensitive with 358.6 µM.

Figure 14. Effect of paclitaxel treatment on endometrial cancer cell lines. Red: resistant, blue: sensitive.

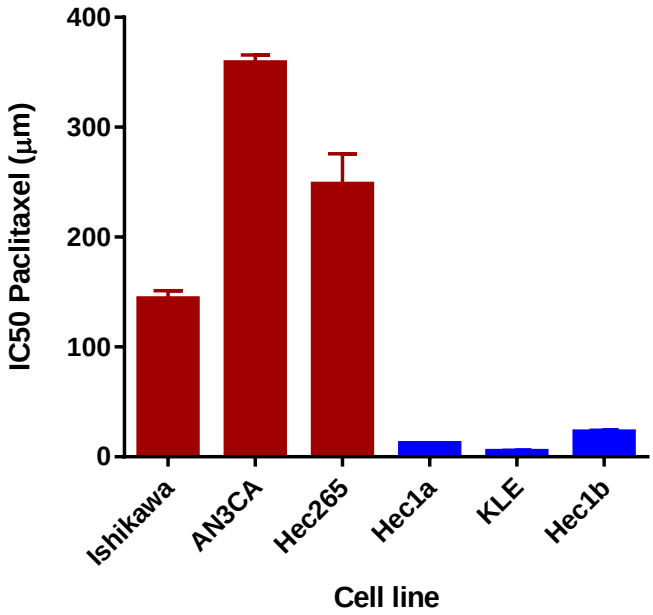

The three cell lines with the highest HRD scores (Hec1a, Hec1b and KLE) were significantly more sensitive to all three agents tested (cisplatin, paclitaxel and olaparib) than were the cell lines with low (Ishikawa) or intermediate HRD score (AN3CA, Hec265). Our *in vitro* findings are similar to previous studies that found higher HRD score predictive of response to platinum chemotherapy in patients with breast cancer.

Effect of olaparib treatment in high HRD score orthotopic model

Effect of olaparib on tumor growth

Hec1a was selected for *in vivo* use due to its high HRD score, wild type BRCA status, and high sensitivity to olaparib. 40 mice nude mice were inoculated with Hec1a cells (4 x 10^6 into the left uterine horn); 10 mice per group were used in order to have adequate power to detect differences between groups. Mice were treated with siRNA targeting BRCA1 (20 mice) or a control sequence (20 mice) (5ug intraperitoneally twice weekly). BRCA1 was selected as a target due to its multiple roles within the DNA damage repair pathways. Within each group, 10 mice were treated with olaparib (50mg/kg daily by oral gavage). In the group receiving control siRNA, treatment with olaparib resulted in a significant reduction in tumor weight (Figure 15-A). In the group receiving BRCA1 siRNA, treatment with olaparib also resulted in a significant reduction in tumor weight (Figure 13-A). The same trend was observed in the number of tumor nodules (Figure 15-B). Treatment with BRCA1 siRNA alone resulted in a significant decrease in tumor weight as compared to control siRNA. There was no significant reduction in mouse weight in any of the treatment groups as compared to controls (Figure 15-C). Figure 15-D demonstrates photos taken at necropsy, with tumors outlined in white.

Figure 15 (A-D). Effect of control or BRCA1 siRNA +/- olaparib on tumor growth in Hec1a model. (A) Tumor weight, (B) Number of tumor nodules, (C) Mouse weight, (D) Representative necropsy pictures. Error bars represent the standard error of the mean (SEM). ***, P < 0.001 and ****, P<0.0001.

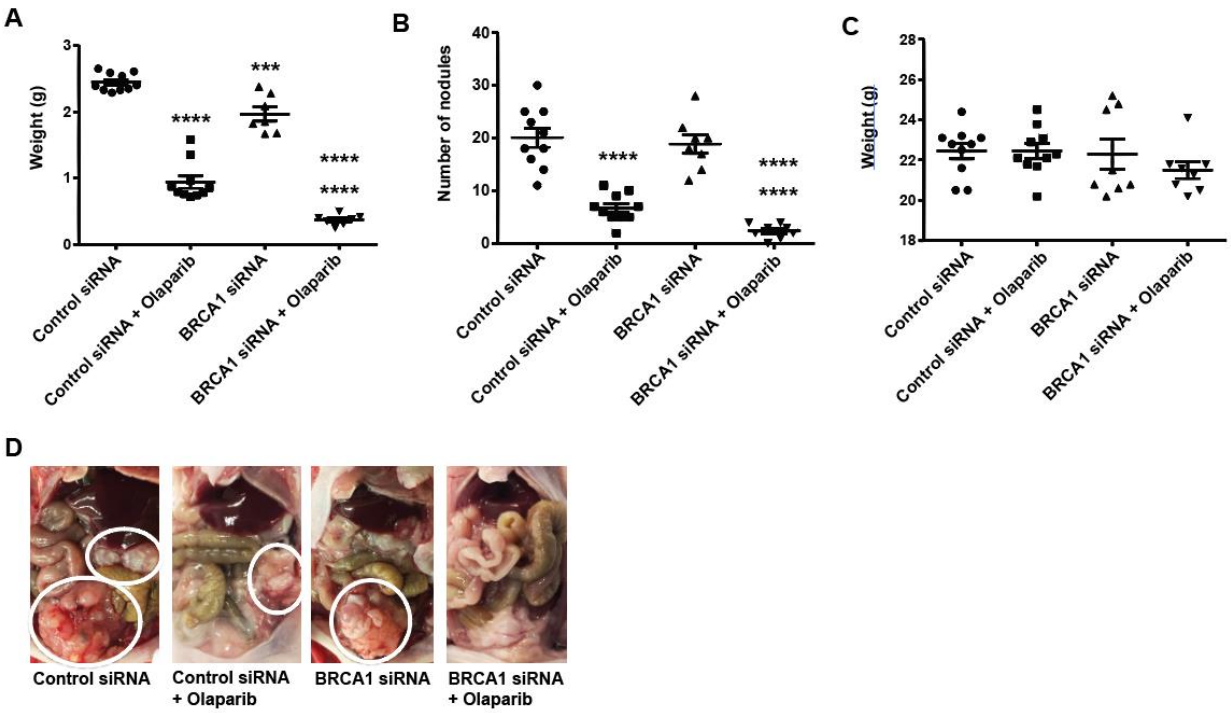

Biological effects of olaparib treatment

Given the differences in tumor growth between groups, we evaluated for biological effects within tumors collected at necropsy. In the group treated with control siRNA, the addition of olaparib to control siRNA resulted in significant reduction in cellular proliferation as determined by Ki67 (Figure 16). Treatment with BRCA1 siRNA alone resulted in significantly increased proliferation as compared to control siRNA. In the group treated with BRCA1 siRNA, addition of olaparib to BRCA1 siRNA resulted in significantly reduced proliferation.

Figure 16. Representative pictures of the four treatment groups after Ki67 staining. Error bars represent SEM. ***, P < 0.001 and ****, P<0.0001.

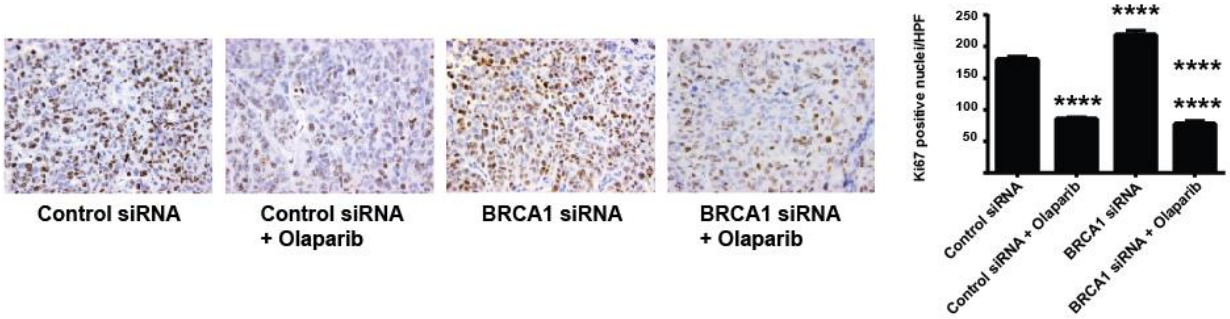

In the group treated with control siRNA, the addition of olaparib to control siRNA resulted in significant increase in apoptosis as determined by cleaved caspase 3 (Figure 17). In the group treated with BRCA1 siRNA, addition of olaparib to BRCA1 siRNA resulted in significantly increased apoptosis.

Figure 17. Representative pictures of the four treatment groups after cleaved caspase 3 staining. Error bars represent SEM. ****, P<0.0001.

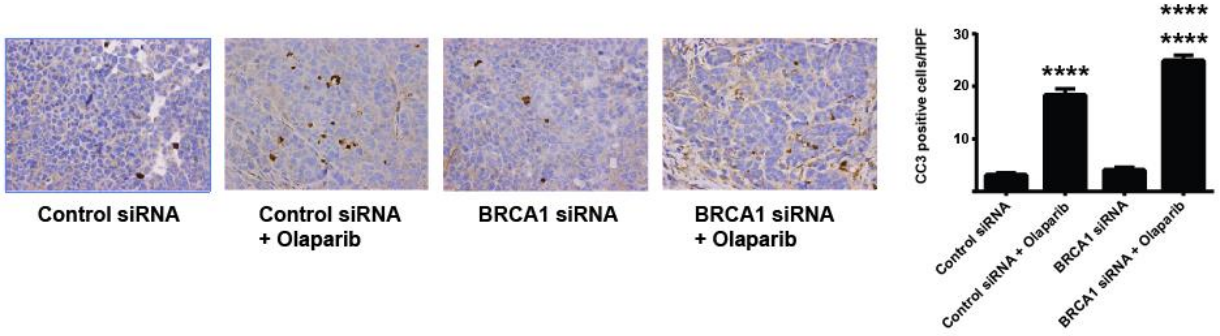

Histone H2AX is phosphorylated in response to DNA double strand breaks and is an early marker for HR function [88]. Phosphorylated H2AX (γ-H2AX) is necessary for both BRCA1 recruitment as well as MRN complex formation at the site of DNA double strand breaks [89,90]. Immunofluorescent staining for γ-H2AX was performed in order to detect differences in the number of double strand breaks between groups (Figure 18). In both siRNA conditions, treatment with olaparib significantly decreased the number of γ-H2AX per cell. This indicates that in the setting of HR deficiency, which we assume based on the HRD score of 19, olaparib further decreases HR function, independent of BRCA1 expression.

Figure 18. Representative pictures of the four treatment groups after H2AX staining. Error bars represent SEM. ****, P<0.0001.

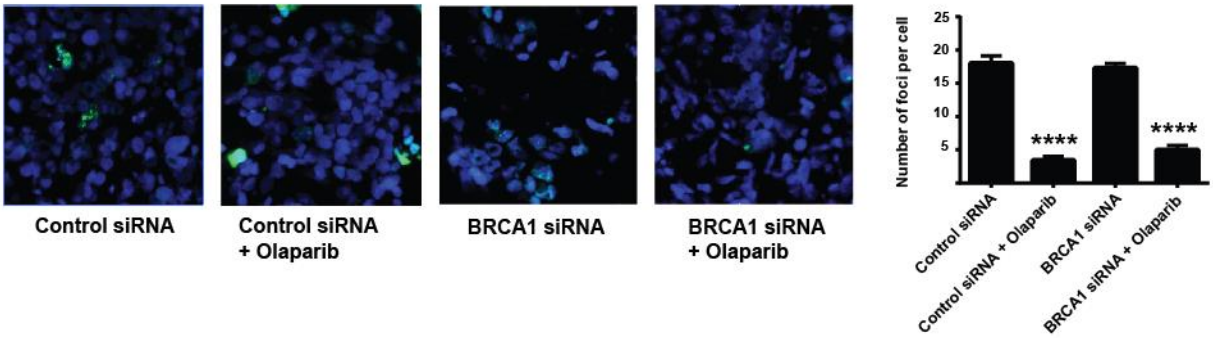

We determined the efficacy of BRCA1 silencing in the four treatment groups (Figure 19, top panel) using tumor samples obtained at the time of necropsy. In the groups treated with BRCA1 siRNA, there was fairly uniform silencing as shown by decreased protein expression. Differences within groups are likely due to tumor heterogeneity. We also determined RAD51 expression in all four groups using tumor samples obtained at the time of necropsy (Figure 19, middle panel). In the two groups treated with olaparib, there is decreased expression of RAD51 as compared to the untreated groups. The panels have equal exposure time. When

the left middle panel (siRNA only) is compared to the right middle panel (siRNA plus olaparib), there is decreased expression of RAD51 in the groups treated with olaparib, indicating that in this model with HR deficiency, olaparib further decreases HR function regardless of BRCA1 expression.

Figure 19. Western blots demonstrating BRCA1 protein expression levels (top panel) and RAD51 protein expression levels (middle panel) across four treatment groups in tumor samples obtained at the time of necropsy. Vinculin was used as a loading control.

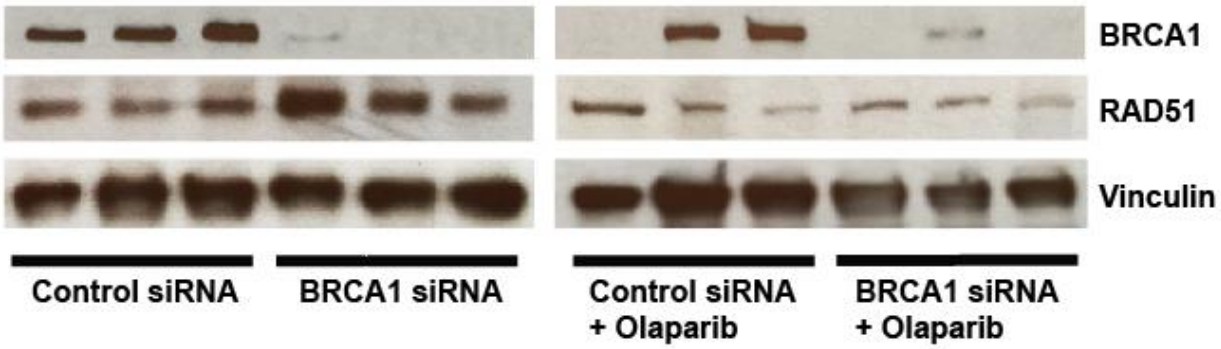

Discussion

The key findings of the work shown here are that HRD scores of 10 or greater are prognostic of poor survival outcomes in patients with advanced endometrial cancer. Our cohort was the first group of endometrial cancer patients to undergo HRD score testing. In an orthotopic mouse model with an HRD score of 19, olaparib treatment significantly decreased tumor growth, proliferation and HR function, regardless of BRCA1 expression status.

The analysis provided here describes the molecular characteristics of a cohort of patients with endometrial cancer who had advanced disease at the time of diagnosis, or who had high risk features noted at the time of initial surgery. While there is not statistical evidence that survival differs between the four molecular subtypes, nor when the group is split between HRD scores above and below 10, there are clear trends toward differences in survival in our cohort. Of particular interest is the group of patients with HRD scores ≥ 10, which comprises 11 patients. Of these, nine patients had mutations in TP53 with LOH of the second allele, and five patients had mutations in PTEN. In this group, the majority had stage III or IV disease and grade 3 histology at the time of diagnosis. Likewise, the three cell lines in our study with the highest HRD scores (Hec1a, Hec1b and KLE) also have missense mutations in TP53. In endometrioid endometrial cancer, mutations in TP53 are more common with increasing grade [91]. The reported rate of rate of TP53 mutations in endometrioid endometrial cancer is 11.4% in the TCGA analysis. In contrast, the rate of TP53 mutations in serous uterine carcinoma is approximately 90% [30] which is comparable to that of high grade serous ovarian cancer [92]. Likewise, approximately 25% of the high grade endometrioid samples in the TCGA analysis had mutational profiles similar to that of uterine serous carcinoma[30], which has a more aggressive clinical course [5]. The group of patients in our cohort with HRD scores ≥ 10 appears resembles uterine serous carcinoma both biologically and clinically.

The mutational characteristics of this subset of tumors provide a possible explanation for their late stage at diagnosis and poor survival outcomes. P53 is activated in response to cellular stress, and p53 levels increase in response to DNA damage, leading to cell-cycle arrest, DNA repair, or apoptosis in cases of irreparable DNA damage [93]. In the absence of normally functioning p53, as in the case of TP53 mutations, cells with DNA damage can continue in the cell cycle, leading to uncontrolled proliferation. In cases where TP53 is mutated, HR deficiency may manifest itself as uncontrolled cellular proliferation secondary to the potentiation of unrepaired DNA damage, ultimately leading to more aggressive disease and shorter survival. Preclinical studies have shown that administration of PARP inhibitors can sensitize TP53 mutated breast cancer cells, likely via increased apoptosis secondary to PARP inhibition [94]. If TP53 mutations do in fact play a role in HR deficiency and the tumor behavior we observe in this group of patients, then PARP inhibitor therapy may prove to be a rational choice.

Likewise, mutations in PTEN have been shown to induce genomic instability by defective RAD51 foci formation, thus inhibiting HR [57,58]. Our *in vitro* work did not demonstrate that PTEN mutations sensitized to PARP inhibitor or platinum chemotherapy, and the majority of PTEN mutations occurred in patients with HRD scores less than 10. If PTEN loss of function does indeed sensitize to PARP inhibition *in vivo*, the two subsets of patients in our cohort with intermediate survival values in which PTEN mutations were common (MSI positive and the group including all others) may also benefit from PARP inhibition.

In our patient cohort, BRCA1 and BRCA2 mutations were uncommon; four patients had BRCA1 mutations and nine patients had BRCA2 mutations. The mutations were generally present in only one allele, indicating BRCA was likely functional. In addition, all of these patient had HRD scores less than five, suggesting that HR deficiency was not present. Our initial

analysis using TCGA data suggested that BRCA mutations did not have a significant impact on survival, and the results from our patient cohort confirm this. Furthermore, our *in vivo* model demonstrates that whether or not BRCA1 is silenced, mice who received olaparib treatment had significantly less tumor growth than controls. We also observed a decrease in RAD51 expression and γ-H2AX foci formation in the groups treated with olaparib, regardless of whether or not BRCA1 was silenced. We postulate that intrinsic HR deficiency in the cell line used, rather than BRCA1 function, affects HR function. The HRD score has been shown to be superior to both clinical variables and BRCA mutation status in identifying likely responders to platinum chemotherapy in breast cancer [77], and there is ample evidence that mutations in genes other than BRCA1 and BRCA2 can produce clinically significant HR deficiency [95,96,97].

Implications and future directions

The HRD score has previously been validated and found to have clinical relevance in both breast and ovarian cancer, and is logistically feasible to perform on FFPE tissue sections [73,77]. Our work demonstrates that a subset of patients with endometrial cancer who had high HRD scores have particularly poor survival in comparison to patients with low HRD scores. While the biology supporting the use of PARP inhibitors in endometrial cancer is less robust than that in breast or ovarian cancer, our *in vivo* work demonstrates that in the setting of HR deficiency, PARP inhibitors are beneficial, regardless of BRCA1 function. This is the first use of the HRD score in a cohort of endometrial cancer patient samples, and of the HRD score in an *in vivo* model of endometrial cancer. Despite promising results thus far, endometrial cancer presents some unique challenges that set it apart from breast and high grade serous ovarian cancer, and therefore, make our findings difficult to interpret in the context of what is known about the HRD score. Endometrioid endometrial cancer is commonly

diagnosed at early stage when tumor is confined to the endometrium, and surgery is generally the first intervention [17]. Except in infrequent cases of widely metastatic disease at the time of diagnosis, or medically inoperable patients, the majority of tumor burden is removed at the time of initial surgery. Because of this, it may be difficult to evaluate response to therapy in the same manner as in breast or ovarian cancer, because response is likely confounded with successful surgical resection in most cases. In breast cancer, improved platinum response is seen in patients with higher HRD scores [77]. We evaluated response to platinum in relation to HRD score in our cohort, and did not find a significant relationship. Moreover, the level of intrinsic HR deficiency in breast and ovarian tumors appears to be higher than in endometrial tumors. The cutoff threshold for high HRD score in breast and ovarian cancer has been established as greater than or equal to 42 after analyzing several data sets totaling over 1000 tumors, including large proportion of BRCA deficient tumors [76,77,98]. In contrast, of the 112 samples in our cohort for which HRD scores were generated, only 10 had HRD scores greater than or equal to 10. Furthermore, our rate of BRCA mutations was very low and likely not clinically significant, as there were no cases of biallelic loss.

The mutational characteristics of the patients with the highest HRD scores indicate that several specific subsets of patients with endometrial cancer may benefit from HRD testing and use of the HRD score to triage into further therapy. First are the patients with endometrioid histology who have stage III or IV disease and/or grade 3 histology. Prior studies have shown similarities between the mutational profile of these tumors and uterine serous tumors [30]. Second, uterine serous tumors have a clinical course, mutational profile, and recommended treatment similar to that of high grade serous ovarian cancer, making this tumor type an ideal candidate for further study in this area [5,30,92]. These patients could benefit from having HRD score information about their tumors for several reasons. First, uterine serous tumors are more likely to present with stage III or IV disease than endometrioid tumors (38% vs 16%,

respectively) and are more likely to recur with distant metastases or carcinomatosis [5]. Because surgical resection may not be feasible in these patients, assessing potential response to platinum is of interest. Second, because of the inherently aggressive nature of the disease, the use of targeted therapies if platinum is ineffective may be warranted. If indeed uterine serous tumors demonstrated a higher level of HR deficiency than endometrioid tumors, PARP inhibitors may be a rational choice for adjuvant therapy.

In conclusion, our work is the first report of the use of the HRD score in endometrial cancer, both in patient samples and in preclinical models. We demonstrated that higher HRD scores were prognostic of worse survival, although not at a statistically significant level. On the basis of this study, further investigation into the use of the HRD score in high risk endometrial cancer subtypes is warranted.

Bibliography

[1] R.L. Siegel, K.D. Miller, A. Jemal, Cancer statistics, 2015, CA Cancer J Clin 65 (2015) 5-29.

[2] F. Amant, P. Moerman, P. Neven, D. Timmerman, E. Van Limbergen, I. Vergote, Endometrial cancer, Lancet 366 (2005) 491-505.

[3] J.L. Hecht, G.L. Mutter, Molecular and pathologic aspects of endometrial carcinogenesis, J Clin Oncol 24 (2006) 4783-4791.

[4] J.V. Bokhman, Two pathogenetic types of endometrial carcinoma, Gynecol Oncol 15 (1983) 10-17.

[5] K.N. Moore, A.N. Fader, Uterine papillary serous carcinoma, Clin Obstet Gynecol 54 (2011) 278-291.

[6] http://seer.cancer.gov/statfacts/html/corp.html (Accessed on May 2, 2016).

[7] S. Furness, H. Roberts, J. Marjoribanks, A. Lethaby, M. Hickey, C. Farquhar, Hormone therapy in postmenopausal women and risk of endometrial hyperplasia, Cochrane Database Syst Rev (2009) CD000402.

[8] J.D. Woodruff, J.H. Pickar, Incidence of endometrial hyperplasia in postmenopausal women taking conjugated estrogens (Premarin) with medroxyprogesterone acetate or conjugated estrogens alone. The Menopause Study Group, Am J Obstet Gynecol 170 (1994) 1213-1223.

[9] S.T. Schumer, S.A. Cannistra, Granulosa cell tumor of the ovary, J Clin Oncol 21 (2003) 1180-1189.

[10] T. Gredmark, S. Kvint, G. Havel, L.A. Mattsson, Adipose tissue distribution in postmenopausal women with adenomatous hyperplasia of the endometrium, Gynecol Oncol 72 (1999) 138-142.

[11] A.R. Folsom, S.A. Kaye, J.D. Potter, R.J. Prineas, Association of incident carcinoma of the endometrium with body weight and fat distribution in older women: early findings of the Iowa Women's Health Study, Cancer Res 49 (1989) 6828-6831.

[12] J. Iqbal, O.M. Ginsburg, T.D. Wijeratne, A. Howell, G. Evans, I. Sestak, S.A. Narod, Endometrial cancer and venous thromboembolism in women under age 50 who take tamoxifen for prevention of breast cancer: a systematic review, Cancer Treat Rev 38 (2012) 318-328.

[13] L.A. Brinton, M.L. Berman, R. Mortel, L.B. Twiggs, R.J. Barrett, G.D. Wilbanks, L. Lannom, R.N. Hoover, Reproductive, menstrual, and medical risk factors for endometrial cancer: results from a case-control study, Am J Obstet Gynecol 167 (1992) 1317-1325.

[14] J.M. Lancaster, C.B. Powell, N.D. Kauff, I. Cass, L.M. Chen, K.H. Lu, D.G. Mutch, A. Berchuck, B.Y. Karlan, T.J. Herzog, C. Society of Gynecologic Oncologists Education, Society of Gynecologic Oncologists Education Committee statement on risk assessment for inherited gynecologic cancer predispositions, Gynecol Oncol 107 (2007) 159-162.

[15] J.S. Kwon, J.L. Scott, C.B. Gilks, M.S. Daniels, C.C. Sun, K.H. Lu, Testing women with endometrial cancer to detect Lynch syndrome, J Clin Oncol 29 (2011) 2247-2252.

[16] R. Pilarski, J.A. Stephens, R. Noss, J.L. Fisher, T.W. Prior, Predicting PTEN mutations: an evaluation of Cowden syndrome and Bannayan-Riley-Ruvalcaba syndrome clinical features, J Med Genet 48 (2011) 505-512.

[17] Practice Bulletin No. 149: Endometrial cancer, Obstet Gynecol 125 (2015) 1006-1026.

[18] J.L. Benedet, H. Bender, H. Jones, 3rd, H.Y. Ngan, S. Pecorelli, FIGO staging classifications and clinical practice guidelines in the management of gynecologic cancers. FIGO Committee on Gynecologic Oncology, Int J Gynaecol Obstet 70 (2000) 209-262.

[19] W.T. Creasman, C.P. Morrow, B.N. Bundy, H.D. Homesley, J.E. Graham, P.B. Heller, Surgical pathologic spread patterns of endometrial cancer. A Gynecologic Oncology Group Study, Cancer 60 (1987) 2035-2041.

[20] R.C. Boronow, C.P. Morrow, W.T. Creasman, P.J. Disaia, S.G. Silverberg, A. Miller, J.A. Blessing, Surgical staging in endometrial cancer: clinical-pathologic findings of a prospective study, Obstet Gynecol 63 (1984) 825-832.

[21] A. Mariani, M.J. Webb, G.L. Keeney, M.G. Haddock, G. Calori, K.C. Podratz, Low-risk corpus cancer: is lymphadenectomy or radiotherapy necessary?, Am J Obstet Gynecol 182 (2000) 1506-1519.

[22] S. Pecorelli, Revised FIGO staging for carcinoma of the vulva, cervix, and endometrium, Int J Gynaecol Obstet 105 (2009) 103-104.

[23] H.M. Keys, J.A. Roberts, V.L. Brunetto, R.J. Zaino, N.M. Spirtos, J.D. Bloss, A. Pearlman, M.A. Maiman, J.G. Bell, G. Gynecologic Oncology, A phase III trial of surgery with or without adjunctive external pelvic radiation therapy in intermediate risk endometrial adenocarcinoma: a Gynecologic Oncology Group study, Gynecol Oncol 92 (2004) 744-751.

[24] R.A. Nout, V.T. Smit, H. Putter, I.M. Jurgenliemk-Schulz, J.J. Jobsen, L.C. Lutgens, E.M. van der Steen-Banasik, J.W. Mens, A. Slot, M.C. Kroese, B.N. van Bunningen, A.C. Ansink, W.L. van Putten, C.L. Creutzberg, P.S. Group, Vaginal brachytherapy versus pelvic external beam radiotherapy for patients with endometrial cancer of high-intermediate risk (PORTEC-2): an open-label, non-inferiority, randomised trial, Lancet 375 (2010) 816-823.

[25] NCCN Clinical Practice Guidelines in Oncology-Uterine Neoplasms (Version 2.2016) https://www.nccn.org/professionals/physician_gls/pdf/uterine.pdf (Accessed May 2, 2016).

[26] P.J. Hoskins, K.D. Swenerton, J.A. Pike, F. Wong, P. Lim, C. Acquino-Parsons, N. Lee, Paclitaxel and carboplatin, alone or with irradiation, in advanced or recurrent endometrial cancer: a phase II study, J Clin Oncol 19 (2001) 4048-4053.

[27] M.G. Del Carmen, D.M. Boruta, 2nd, J.O. Schorge, Recurrent endometrial cancer, Clin Obstet Gynecol 54 (2011) 266-277.

[28] J.T. Thigpen, M.F. Brady, R.D. Alvarez, M.D. Adelson, H.D. Homesley, A. Manetta, J.T. Soper, F.T. Given, Oral medroxyprogesterone acetate in the treatment of advanced or recurrent endometrial carcinoma: a dose-response study by the Gynecologic Oncology Group, J Clin Oncol 17 (1999) 1736-1744.

[29] R.R. Barakat, N.A. Goldman, D.A. Patel, E.S. Venkatraman, J.P. Curtin, Pelvic exenteration for recurrent endometrial cancer, Gynecol Oncol 75 (1999) 99-102.

[30] N. Cancer Genome Atlas Research, C. Kandoth, N. Schultz, A.D. Cherniack, R. Akbani, Y. Liu, H. Shen, A.G. Robertson, I. Pashtan, R. Shen, C.C. Benz, C. Yau, P.W. Laird, L. Ding, W. Zhang, G.B. Mills, R. Kucherlapati, E.R. Mardis, D.A. Levine, Integrated genomic characterization of endometrial carcinoma, Nature 497 (2013) 67-73.

[31] G.L. Mutter, M.C. Lin, J.T. Fitzgerald, J.B. Kum, J.P. Baak, J.A. Lees, L.P. Weng, C. Eng, Altered PTEN expression as a diagnostic marker for the earliest endometrial precancers, J Natl Cancer Inst 92 (2000) 924-930.

[32] H.T. Lynch, A. de la Chapelle, Hereditary colorectal cancer, N Engl J Med 348 (2003) 919-932.

[33] L.A. Meyer, R.R. Broaddus, K.H. Lu, Endometrial cancer and Lynch syndrome: clinical and pathologic considerations, Cancer Control 16 (2009) 14-22.

[34] M. Esteller, R. Levine, S.B. Baylin, L.H. Ellenson, J.G. Herman, MLH1 promoter hypermethylation is associated with the microsatellite instability phenotype in sporadic endometrial carcinomas, Oncogene 17 (1998) 2413-2417.

[35] T. Koessler, M.Z. Oestergaard, H. Song, J. Tyrer, B. Perkins, A.M. Dunning, D.F. Easton, P.D. Pharoah, Common variants in mismatch repair genes and risk of colorectal cancer, Gut 57 (2008) 1097-1101.

[36] D. Black, R.A. Soslow, D.A. Levine, C. Tornos, S.C. Chen, A.J. Hummer, F. Bogomolniy, N. Olvera, R.R. Barakat, J. Boyd, Clinicopathologic significance of defective DNA mismatch repair in endometrial carcinoma, J Clin Oncol 24 (2006) 1745-1753.

[37] G. Choe, S. Horvath, T.F. Cloughesy, K. Crosby, D. Seligson, A. Palotie, L. Inge, B.L. Smith, C.L. Sawyers, P.S. Mischel, Analysis of the phosphatidylinositol 3'-kinase signaling pathway in glioblastoma patients in vivo, Cancer Res 63 (2003) 2742-2746.

[38] K. Oda, D. Stokoe, Y. Taketani, F. McCormick, High frequency of coexistent mutations of PIK3CA and PTEN genes in endometrial carcinoma, Cancer Res 65 (2005) 10669-10673.

[39] B.M. Slomovitz, R.L. Coleman, The PI3K/AKT/mTOR pathway as a therapeutic target in endometrial cancer, Clin Cancer Res 18 (2012) 5856-5864.

[40] B.M. Slomovitz, K.H. Lu, T. Johnston, R.L. Coleman, M. Munsell, R.R. Broaddus, C. Walker, L.M. Ramondetta, T.W. Burke, D.M. Gershenson, J. Wolf, A phase 2 study of the oral mammalian target of rapamycin inhibitor, everolimus, in patients with recurrent endometrial carcinoma, Cancer 116 (2010) 5415-5419.

[41] I. Ray-Coquard, L. Favier, B. Weber, C. Roemer-Becuwe, P. Bougnoux, M. Fabbro, A. Floquet, F. Joly, A. Plantade, D. Paraiso, E. Pujade-Lauraine, Everolimus as second- or third-line treatment of advanced endometrial cancer: ENDORAD, a phase II trial of GINECO, Br J Cancer 108 (2013) 1771-1777.

[42] B.M. Slomovitz, Y. Jiang, M.S. Yates, P.T. Soliman, T. Johnston, M. Nowakowski, C. Levenback, Q. Zhang, K. Ring, M.F. Munsell, D.M. Gershenson, K.H. Lu, R.L.

Coleman, Phase II study of everolimus and letrozole in patients with recurrent endometrial carcinoma, J Clin Oncol 33 (2015) 930-936.

[43] A.A. Kamat, W.M. Merritt, D. Coffey, Y.G. Lin, P.R. Patel, R. Broaddus, E. Nugent, L.Y. Han, C.N. Landen, Jr., W.A. Spannuth, C. Lu, R.L. Coleman, D.M. Gershenson, A.K. Sood, Clinical and biological significance of vascular endothelial growth factor in endometrial cancer, Clin Cancer Res 13 (2007) 7487-7495.

[44] C. Aghajanian, M.W. Sill, K.M. Darcy, B. Greer, D.S. McMeekin, P.G. Rose, J. Rotmensch, M.N. Barnes, P. Hanjani, K.K. Leslie, Phase II trial of bevacizumab in recurrent or persistent endometrial cancer: a Gynecologic Oncology Group study, J Clin Oncol 29 (2011) 2259-2265.

[45] D. Bender, M.W. Sill, H.A. Lankes, H.D. Reyes, C.J. Darus, J.E. Delmore, J. Rotmensch, H.J. Gray, R.S. Mannel, J.M. Schilder, M.I. Hunter, C.K. McCourt, M.I. Samuelson, K.K. Leslie, A phase II evaluation of cediranib in the treatment of recurrent or persistent endometrial cancer: An NRG Oncology/Gynecologic Oncology Group study, Gynecol Oncol 138 (2015) 507-512.

[46] B.B. Zhou, S.J. Elledge, The DNA damage response: putting checkpoints in perspective, Nature 408 (2000) 433-439.

[47] J.F. Ward, Radiation mutagenesis: the initial DNA lesions responsible, Radiat Res 142 (1995) 362-368.

[48] J.H. Lee, T.T. Paull, ATM activation by DNA double-strand breaks through the Mre11-Rad50-Nbs1 complex, Science 308 (2005) 551-554.

[49] D. Cortez, Y. Wang, J. Qin, S.J. Elledge, Requirement of ATM-dependent phosphorylation of brca1 in the DNA damage response to double-strand breaks, Science 286 (1999) 1162-1166.

[50] R. Scully, J. Chen, A. Plug, Y. Xiao, D. Weaver, J. Feunteun, T. Ashley, D.M. Livingston, Association of BRCA1 with Rad51 in mitotic and meiotic cells, Cell 88 (1997) 265-275.

[51] P. Baumann, S.C. West, Role of the human RAD51 protein in homologous recombination and double-stranded-break repair, Trends Biochem Sci 23 (1998) 247-251.

[52] M.E. Moynahan, J.W. Chiu, B.H. Koller, M. Jasin, Brca1 controls homology-directed DNA repair, Mol Cell 4 (1999) 511-518.

[53] A. Tutt, A. Ashworth, The relationship between the roles of BRCA genes in DNA repair and cancer predisposition, Trends Mol Med 8 (2002) 571-576.

[54] Q. Zhong, C.F. Chen, S. Li, Y. Chen, C.C. Wang, J. Xiao, P.L. Chen, Z.D. Sharp, W.H. Lee, Association of BRCA1 with the hRad50-hMre11-p95 complex and the DNA damage response, Science 285 (1999) 747-750.

[55] M.E. Moynahan, A.J. Pierce, M. Jasin, BRCA2 is required for homology-directed repair of chromosomal breaks, Mol Cell 7 (2001) 263-272.

[56] A. Tutt, D. Bertwistle, J. Valentine, A. Gabriel, S. Swift, G. Ross, C. Griffin, J. Thacker, A. Ashworth, Mutation in Brca2 stimulates error-prone homology-directed repair of DNA double-strand breaks occurring between repeated sequences, EMBO J 20 (2001) 4704-4716.

[57] W.H. Shen, A.S. Balajee, J. Wang, H. Wu, C. Eng, P.P. Pandolfi, Y. Yin, Essential role for nuclear PTEN in maintaining chromosomal integrity, Cell 128 (2007) 157-170.

[58] K.J. Dedes, D. Wetterskog, A.M. Mendes-Pereira, R. Natrajan, M.B. Lambros, F.C. Geyer, R. Vatcheva, K. Savage, A. Mackay, C.J. Lord, A. Ashworth, J.S. Reis-Filho, PTEN deficiency in endometrioid endometrial adenocarcinomas predicts sensitivity to PARP inhibitors, Sci Transl Med 2 (2010) 53ra75.

[59] K. Kurose, X.P. Zhou, T. Araki, S.A. Cannistra, E.R. Maher, C. Eng, Frequent loss of PTEN expression is linked to elevated phosphorylated Akt levels, but not associated with p27 and cyclin D1 expression, in primary epithelial ovarian carcinomas, Am J Pathol 158 (2001) 2097-2106.

[60] L. Salmena, A. Carracedo, P.P. Pandolfi, Tenets of PTEN tumor suppression, Cell 133 (2008) 403-414.

[61] A. Antoniou, P.D. Pharoah, S. Narod, H.A. Risch, J.E. Eyfjord, J.L. Hopper, N. Loman, H. Olsson, O. Johannsson, A. Borg, B. Pasini, P. Radice, S. Manoukian, D.M. Eccles, N. Tang, E. Olah, H. Anton-Culver, E. Warner, J. Lubinski, J. Gronwald, B. Gorski, H. Tulinius, S. Thorlacius, H. Eerola, H. Nevanlinna, K. Syrjakoski, O.P. Kallioniemi, D. Thompson, C. Evans, J. Peto, F. Lalloo, D.G. Evans, D.F. Easton, Average risks of breast and ovarian cancer associated with BRCA1 or BRCA2 mutations detected in case Series unselected for family history: a combined analysis of 22 studies, Am J Hum Genet 72 (2003) 1117-1130.

[62] S. Chen, G. Parmigiani, Meta-analysis of BRCA1 and BRCA2 penetrance, J Clin Oncol 25 (2007) 1329-1333.

[63] N. Mavaddat, S. Peock, D. Frost, S. Ellis, R. Platte, E. Fineberg, D.G. Evans, L. Izatt, R.A. Eeles, J. Adlard, R. Davidson, D. Eccles, T. Cole, J. Cook, C. Brewer, M. Tischkowitz, F. Douglas, S. Hodgson, L. Walker, M.E. Porteous, P.J. Morrison, L.E. Side, M.J. Kennedy, C. Houghton, A. Donaldson, M.T. Rogers, H. Dorkins, Z. Miedzybrodzka, H. Gregory, J. Eason, J. Barwell, E. McCann, A. Murray, A.C. Antoniou, D.F. Easton, Embrace, Cancer risks for BRCA1 and BRCA2 mutation carriers: results from prospective analysis of EMBRACE, J Natl Cancer Inst 105 (2013) 812-822.

[64] M.S. Satoh, T. Lindahl, Role of poly(ADP-ribose) formation in DNA repair, Nature 356 (1992) 356-358.

[65] N. Schultz, E. Lopez, N. Saleh-Gohari, T. Helleday, Poly(ADP-ribose) polymerase (PARP-1) has a controlling role in homologous recombination, Nucleic Acids Res 31 (2003) 4959-4964.

[66] H. Farmer, N. McCabe, C.J. Lord, A.N. Tutt, D.A. Johnson, T.B. Richardson, M. Santarosa, K.J. Dillon, I. Hickson, C. Knights, N.M. Martin, S.P. Jackson, G.C. Smith, A. Ashworth, Targeting the DNA repair defect in BRCA mutant cells as a therapeutic strategy, Nature 434 (2005) 917-921.

[67] H.E. Bryant, N. Schultz, H.D. Thomas, K.M. Parker, D. Flower, E. Lopez, S. Kyle, M. Meuth, N.J. Curtin, T. Helleday, Specific killing of BRCA2-deficient tumours with inhibitors of poly(ADP-ribose) polymerase, Nature 434 (2005) 913-917.

[68] M.D. Forster, K.J. Dedes, S. Sandhu, S. Frentzas, R. Kristeleit, A. Ashworth, C.J. Poole, B. Weigelt, S.B. Kaye, L.R. Molife, Treatment with olaparib in a patient with PTEN-deficient endometrioid endometrial cancer, Nat Rev Clin Oncol 8 (2011) 302-306.

[69] A. Tutt, M. Robson, J.E. Garber, S.M. Domchek, M.W. Audeh, J.N. Weitzel, M. Friedlander, B. Arun, N. Loman, R.K. Schmutzler, A. Wardley, G. Mitchell, H. Earl, M. Wickens, J. Carmichael, Oral poly(ADP-ribose) polymerase inhibitor olaparib in patients with BRCA1 or BRCA2 mutations and advanced breast cancer: a proof-of-concept trial, Lancet 376 (2010) 235-244.

[70] M.W. Audeh, J. Carmichael, R.T. Penson, M. Friedlander, B. Powell, K.M. Bell-McGuinn, C. Scott, J.N. Weitzel, A. Oaknin, N. Loman, K. Lu, R.K. Schmutzler, U. Matulonis, M. Wickens, A. Tutt, Oral poly(ADP-ribose) polymerase inhibitor olaparib in patients with BRCA1 or BRCA2 mutations and recurrent ovarian cancer: a proof-of-concept trial, Lancet 376 (2010) 245-251.

[71] J. Ledermann, P. Harter, C. Gourley, M. Friedlander, I. Vergote, G. Rustin, C.L. Scott, W. Meier, R. Shapira-Frommer, T. Safra, D. Matei, A. Fielding, S. Spencer, B. Dougherty, M. Orr, D. Hodgson, J.C. Barrett, U. Matulonis, Olaparib maintenance

therapy in patients with platinum-sensitive relapsed serous ovarian cancer: a preplanned retrospective analysis of outcomes by BRCA status in a randomised phase 2 trial, Lancet Oncol 15 (2014) 852-861.

[72] N. McCabe, N.C. Turner, C.J. Lord, K. Kluzek, A. Bialkowska, S. Swift, S. Giavara, M.J. O'Connor, A.N. Tutt, M.Z. Zdzienicka, G.C. Smith, A. Ashworth, Deficiency in the repair of DNA damage by homologous recombination and sensitivity to poly(ADP-ribose) polymerase inhibition, Cancer Res 66 (2006) 8109-8115.

[73] V. Abkevich, K.M. Timms, B.T. Hennessy, J. Potter, M.S. Carey, L.A. Meyer, K. Smith-McCune, R. Broaddus, K.H. Lu, J. Chen, T.V. Tran, D. Williams, D. Iliev, S. Jammulapati, L.M. FitzGerald, T. Krivak, J.A. DeLoia, A. Gutin, G.B. Mills, J.S. Lanchbury, Patterns of genomic loss of heterozygosity predict homologous recombination repair defects in epithelial ovarian cancer, Br J Cancer 107 (2012) 1776-1782.

[74] N.J. Birkbak, Z.C. Wang, J.Y. Kim, A.C. Eklund, Q. Li, R. Tian, C. Bowman-Colin, Y. Li, A. Greene-Colozzi, J.D. Iglehart, N. Tung, P.D. Ryan, J.E. Garber, D.P. Silver, Z. Szallasi, A.L. Richardson, Telomeric allelic imbalance indicates defective DNA repair and sensitivity to DNA-damaging agents, Cancer Discov 2 (2012) 366-375.

[75] T. Popova, E. Manie, G. Rieunier, V. Caux-Moncoutier, C. Tirapo, T. Dubois, O. Delattre, B. Sigal-Zafrani, M. Bollet, M. Longy, C. Houdayer, X. Sastre-Garau, A. Vincent-Salomon, D. Stoppa-Lyonnet, M.H. Stern, Ploidy and large-scale genomic instability consistently identify basal-like breast carcinomas with BRCA1/2 inactivation, Cancer Res 72 (2012) 5454-5462.

[76] K.M. Timms, V. Abkevich, E. Hughes, C. Neff, J. Reid, B. Morris, S. Kalva, J. Potter, T.V. Tran, J. Chen, D. Iliev, Z. Sangale, E. Tikishvili, M. Perry, A. Zharkikh, A. Gutin, J.S. Lanchbury, Association of BRCA1/2 defects with genomic scores predictive of

DNA damage repair deficiency among breast cancer subtypes, Breast Cancer Res 16 (2014) 475.

[77] M.L. Telli, K.M. Timms, J.E. Reid, B. Hennessy, G.B. Mills, K.C. Jensen, Z. Szallasi, W.T. Barry, E.P. Winer, N. Tung, S.J. Isakoff, P.D. Ryan, A. Greene-Colozzi, A. Gutin, Z. Sangale, D. Iliev, C. Neff, V. Abkevich, J.T. Jones, J.S. Lanchbury, A.R. Hartman, J.E. Garber, J.M. Ford, D.P. Silver, A.L. Richardson, Homologous Recombination Deficiency (HRD) Score Predicts Response to Platinum-Containing Neoadjuvant Chemotherapy in Patients with Triple Negative Breast Cancer, Clin Cancer Res (2016).

[78] R.A. Previs, G.N. Armaiz-Pena, Y.G. Lin, A.N. Davis, S. Pradeep, H.J. Dalton, J.M. Hansen, W.M. Merritt, A.M. Nick, R.R. Langley, R.L. Coleman, A.K. Sood, Dual Metronomic Chemotherapy with Nab-Paclitaxel and Topotecan Has Potent Antiangiogenic Activity in Ovarian Cancer, Mol Cancer Ther 14 (2015) 2677-2686.

[79] R. Rupaimoole, S.Y. Wu, S. Pradeep, C. Ivan, C.V. Pecot, K.M. Gharpure, A.S. Nagaraja, G.N. Armaiz-Pena, M. McGuire, B. Zand, H.J. Dalton, J. Filant, J.B. Miller, C. Lu, N.C. Sadaoui, L.S. Mangala, M. Taylor, T. van den Beucken, E. Koch, C. Rodriguez-Aguayo, L. Huang, M. Bar-Eli, B.G. Wouters, M. Radovich, M. Ivan, G.A. Calin, W. Zhang, G. Lopez-Berestein, A.K. Sood, Hypoxia-mediated downregulation of miRNA biogenesis promotes tumour progression, Nat Commun 5 (2014) 5202.

[80] C.N. Landen, M.S. Kinch, A.K. Sood, EphA2 as a target for ovarian cancer therapy, Expert Opin Ther Targets 9 (2005) 1179-1187.

[81] C.V. Pecot, R. Rupaimoole, D. Yang, R. Akbani, C. Ivan, C. Lu, S. Wu, H.D. Han, M.Y. Shah, C. Rodriguez-Aguayo, J. Bottsford-Miller, Y. Liu, S.B. Kim, A. Unruh, V. Gonzalez-Villasana, L. Huang, B. Zand, M. Moreno-Smith, L.S. Mangala, M. Taylor, H.J. Dalton, V. Sehgal, Y. Wen, Y. Kang, K.A. Baggerly, J.S. Lee, P.T. Ram, M.K. Ravoori, V. Kundra, X. Zhang, R. Ali-Fehmi, A.M. Gonzalez-Angulo, P.P. Massion,

G.A. Calin, G. Lopez-Berestein, W. Zhang, A.K. Sood, Tumour angiogenesis regulation by the miR-200 family, Nat Commun 4 (2013) 2427.

[82] P.H. Thaker, M. Deavers, J. Celestino, A. Thornton, M.S. Fletcher, C.N. Landen, M.S. Kinch, P.A. Kiener, A.K. Sood, EphA2 expression is associated with aggressive features in ovarian carcinoma, Clin Cancer Res 10 (2004) 5145-5150.

[83] S. Pradeep, S.W. Kim, S.Y. Wu, M. Nishimura, P. Chaluvally-Raghavan, T. Miyake, C.V. Pecot, S.J. Kim, H.J. Choi, F.Z. Bischoff, J.A. Mayer, L. Huang, A.M. Nick, C.S. Hall, C. Rodriguez-Aguayo, B. Zand, H.J. Dalton, T. Arumugam, H.J. Lee, H.D. Han, M.S. Cho, R. Rupaimoole, L.S. Mangala, V. Sehgal, S.C. Oh, J. Liu, J.S. Lee, R.L. Coleman, P. Ram, G. Lopez-Berestein, I.J. Fidler, A.K. Sood, Hematogenous metastasis of ovarian cancer: rethinking mode of spread, Cancer Cell 26 (2014) 77-91.

[84] U. Kortmann, J.N. McAlpine, H. Xue, J. Guan, G. Ha, S. Tully, S. Shafait, A. Lau, A.N. Cranston, M.J. O'Connor, D.G. Huntsman, Y. Wang, C.B. Gilks, Tumor growth inhibition by olaparib in BRCA2 germline-mutated patient-derived ovarian cancer tissue xenografts, Clin Cancer Res 17 (2011) 783-791.

[85] J.M. Senra, B.A. Telfer, K.E. Cherry, C.M. McCrudden, D.G. Hirst, M.J. O'Connor, S.R. Wedge, I.J. Stratford, Inhibition of PARP-1 by olaparib (AZD2281) increases the radiosensitivity of a lung tumor xenograft, Mol Cancer Ther 10 (2011) 1949-1958.

[86] V.J. Weston, C.E. Oldreive, A. Skowronska, D.G. Oscier, G. Pratt, M.J. Dyer, G. Smith, J.E. Powell, Z. Rudzki, P. Kearns, P.A. Moss, A.M. Taylor, T. Stankovic, The PARP inhibitor olaparib induces significant killing of ATM-deficient lymphoid tumor cells in vitro and in vivo, Blood 116 (2010) 4578-4587.

[87] S. Pradeep, J. Huang, E.M. Mora, A.M. Nick, M.S. Cho, S.Y. Wu, K. Noh, C.V. Pecot, R. Rupaimoole, M.A. Stein, S. Brock, Y. Wen, C. Xiong, K. Gharpure, J.M. Hansen, A.S. Nagaraja, R.A. Previs, P. Vivas-Mejia, H.D. Han, W. Hu, L.S. Mangala, B. Zand,

L.J. Stagg, J.E. Ladbury, B. Ozpolat, S.N. Alpay, M. Nishimura, R.L. Stone, K. Matsuo, G.N. Armaiz-Pena, H.J. Dalton, C. Danes, B. Goodman, C. Rodriguez-Aguayo, C. Kruger, A. Schneider, S. Haghpeykar, P. Jaladurgam, M.C. Hung, R.L. Coleman, J. Liu, C. Li, D. Urbauer, G. Lopez-Berestein, D.B. Jackson, A.K. Sood, Erythropoietin Stimulates Tumor Growth via EphB4, Cancer Cell 28 (2015) 610-622.

[88] D.R. Pilch, O.A. Sedelnikova, C. Redon, A. Celeste, A. Nussenzweig, W.M. Bonner, Characteristics of gamma-H2AX foci at DNA double-strand breaks sites, Biochem Cell Biol 81 (2003) 123-129.

[89] A. Celeste, S. Petersen, P.J. Romanienko, O. Fernandez-Capetillo, H.T. Chen, O.A. Sedelnikova, B. Reina-San-Martin, V. Coppola, E. Meffre, M.J. Difilippantonio, C. Redon, D.R. Pilch, A. Olaru, M. Eckhaus, R.D. Camerini-Otero, L. Tessarollo, F. Livak, K. Manova, W.M. Bonner, M.C. Nussenzweig, A. Nussenzweig, Genomic instability in mice lacking histone H2AX, Science 296 (2002) 922-927.

[90] R.S. Maser, K.J. Monsen, B.E. Nelms, J.H. Petrini, hMre11 and hRad50 nuclear foci are induced during the normal cellular response to DNA double-strand breaks, Mol Cell Biol 17 (1997) 6087-6096.

[91] S.F. Lax, B. Kendall, H. Tashiro, R.J. Slebos, L. Hedrick, The frequency of p53, K-ras mutations, and microsatellite instability differs in uterine endometrioid and serous carcinoma: evidence of distinct molecular genetic pathways, Cancer 88 (2000) 814-824.

[92] N. Cancer Genome Atlas Research, Integrated genomic analyses of ovarian carcinoma, Nature 474 (2011) 609-615.

[93] N.D. Lakin, S.P. Jackson, Regulation of p53 in response to DNA damage, Oncogene 18 (1999) 7644-7655.

[94] J.A. Munoz-Gamez, D. Martin-Oliva, R. Aguilar-Quesada, A. Canuelo, M.I. Nunez, M.T. Valenzuela, J.M. Ruiz de Almodovar, G. De Murcia, F.J. Oliver, PARP inhibition

sensitizes p53-deficient breast cancer cells to doxorubicin-induced apoptosis, Biochem J 386 (2005) 119-125.

[95] S. Casadei, B.M. Norquist, T. Walsh, S. Stray, J.B. Mandell, M.K. Lee, J.A. Stamatoyannopoulos, M.C. King, Contribution of inherited mutations in the BRCA2-interacting protein PALB2 to familial breast cancer, Cancer Res 71 (2011) 2222-2229.

[96] Z.B. Jenner, A.K. Sood, R.L. Coleman, Evaluation of rucaparib and companion diagnostics in the PARP inhibitor landscape for recurrent ovarian cancer therapy, Future Oncol (2016).

[97] F.W. Liu, K.S. Tewari, New Targeted Agents in Gynecologic Cancers: Synthetic Lethality, Homologous Recombination Deficiency, and PARP Inhibitors, Curr Treat Options Oncol 17 (2016) 12.

[98] B.T. Hennessy, K.M. Timms, M.S. Carey, A. Gutin, L.A. Meyer, D.D. Flake, 2nd, V. Abkevich, J. Potter, D. Pruss, P. Glenn, Y. Li, J. Li, A.M. Gonzalez-Angulo, K.S. McCune, M. Markman, R.R. Broaddus, J.S. Lanchbury, K.H. Lu, G.B. Mills, Somatic mutations in BRCA1 and BRCA2 could expand the number of patients that benefit from poly (ADP ribose) polymerase inhibitors in ovarian cancer, J Clin Oncol 28 (2010) 3570-3576.

Vita

Jean Marie Hansen was born in Royal Oak, Michigan on November 6, 1984, the first daughter of John and Isabel Hansen. After graduating from high school at the International Academy in Bloomfield Hills, Michigan in 2002, she began undergraduate work at the University of Michigan in Ann Arbor, Michigan. She received a Bachelor of Science with a double major in Anthropology-Zoology and Biopsychology & Cognitive Science in April 2006. She attended A.T. Still University—Kirksville College of Osteopathic Medicine and graduated with a Doctor of Osteopathic Medicine in 2010. She then entered the Obstetrics and Gynecology residency program at the University of Iowa Hospitals and Clinics in Iowa City, Iowa, completing her training in 2014. In July 2014, she began a fellowship in Gynecologic Oncology at the University of Texas MD Anderson Cancer Center. Her two year Master of Science program during this fellowship was mentored by Dr. Anil Sood. Her research focused on the clinical significance of homologous recombination deficiency in endometrial cancer with a secondary focus on the role of Notch pathway alterations in endometrial cancer.

Permanent address:

2455 Dunstan Rd, Apt 622

Houston, TX 77005